Stable Concurrent Synchronization in Dynamic System Networks

Quang-Cuong Pham [a] Jean-Jacques Slotine [b]

[a] *Département d'Informatique, École Normale Supérieure, 45 rue d'Ulm, 75005 Paris, France*

[b] *Nonlinear Systems Laboratory, Massachusetts Institute of Technology, Cambridge, MA 02139, USA*

Abstract

In a network of dynamical systems, concurrent synchronization is a regime where multiple groups of fully synchronized elements coexist. In the brain, concurrent synchronization may occur at several scales, with multiple "rhythms" interacting and functional assemblies combining neural oscillators of many different types. Mathematically, stable concurrent synchronization corresponds to convergence to a flow-invariant linear subspace of the global state space. We derive a general condition for such convergence to occur globally and exponentially. We also show that, under mild conditions, global convergence to a concurrently synchronized regime is preserved under basic system combinations such as negative feedback or hierarchies, so that stable concurrently synchronized aggregates of arbitrary size can be constructed. Robustnesss of stable concurrent synchronization to variations in individual dynamics is also quantified. Simple applications of these results to classical questions in systems neuroscience and robotics are discussed.

Key words: synchronization, global exponential stability, contraction theory

Email addresses: cuong.pham@ens.fr (Quang-Cuong Pham), jjs@mit.edu (Jean-Jacques Slotine).

1 Introduction

Distributed synchronization phenomena are the subject of intense research. In the brain, such phenomena are known to occur at different scales, and are heavily studied at both the anatomical and computational levels. In particular, synchronization has been proposed as a general principle for temporal binding of multisensory data [42,13,25,30,47,23,32], and as a mechanism for perceptual grouping [51], neural computation [3,1,50] and neural communication [21,17,39,40]. Similar mathematical models describe fish schooling or certain types of phase-transition in physics [45].

In an ensemble of dynamical elements, *concurrent synchronization* is defined as a regime where the whole system is divided into multiple groups of fully synchronized elements [1] , but elements from different groups are not necessarily synchronized [2,52,36] and can be of entirely different dynamics [11]. It can be easily shown that such a regime corresponds to a flow-invariant linear subspace of the global state space. Concurrent synchronization phenomena are likely pervasive in the brain, where multiple "rhythms" are known to coexist [21,39], neurons can exhibit many qualitatively different types of oscillations [21,16], and functional models often combine multiple oscillatory dynamics.

In this paper, we introduce a simple sufficient condition for a general dynamical system to converge to a flow-invariant subspace. Our analysis is built upon nonlinear contraction theory [27,48], and thus it inherits many of the theory's features :

- global exponential convergence and stability are guaranteed,
- convergence rates can be explicitly computed as eigenvalues of well-defined symmetric matrices,
- robustness to variations in dynamics can be easily quantified,
- under simple conditions, convergence to a concurrently synchronized state can be preserved through system combinations.

As we shall see, under simple conditions on the coupling strengths, architectural symmetries [12] and/or diffusion-like couplings *create globally stable concurrent synchronization phenomena*. This is illustrated in figure 1, which is very loosely inspired by oscillations in the thalamocortical system [25,42,23,32,39]. Qualitatively, global stability of the concurrent synchronization is in the same sense that an equilibrium point is globally stable – any initial conditions will lead back to it, in an exponential fashion. But of course it can yield extremely complex, coordinated behaviors.

[1] In the literature, this phenomenon is often called *poly-*, or *cluster* or *partial* synchronization. However, the last term can also designate a regime where the elements are not fully synchronized but behave coherently [45].

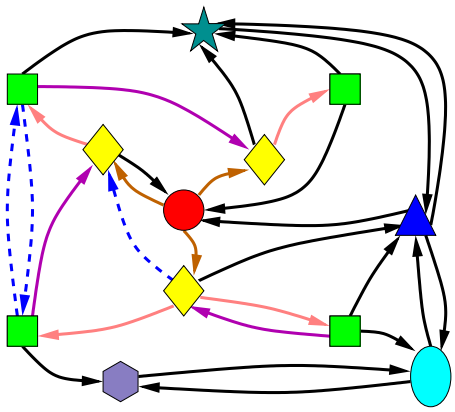

Fig. 1. An example of concurrent synchronization. Systems and connections of the same shape (and color) have identical dynamics (except black arrows, which represent arbitrary connections, and dashed arrows, which represent diffusive connections). This paper shows that under simple conditions on the coupling strengths, the group of (green) squares globally exponentially synchronizes (thus providing synchronized input to the outer elements), and so does the group of (yellow) diamonds, regardless of the specific dynamics, connections, or inputs of the other systems.

Section 2 recalls key concepts of nonlinear contraction theory and derives a theoretical tool for studying global convergence to a flow-invariant subspace. Section 3 presents the paper's main mathematical results, relating stable concurrent synchronization to coupling structures and flow-invariant subspaces created by symmetries or diffusion-like couplings. Robustnesss of concurrent synchronization to variations in individual dynamics is also quantified, showing in particular how approximate symmetries lead to quasi-synchronization. Section 4, motivated by evolution and development, studies conditions under which concurrent synchronization can be preserved through combinations of multiple concurrently synchronized regimes. Finally, section 5 discusses potential applications of these results to general questions in systems neuroscience and robotics.

2 Basic Tools

2.1 Nonlinear contraction theory

This section reviews basic results of nonlinear contraction theory [27,28,43,48], which is the main stability analysis tool used in the paper. Essentially, a nonlinear time-varying dynamic system will be called *contracting* if initial conditions or temporary disturbances are forgotten exponentially fast, i.e., if trajectories of the perturbed system return to their nominal behavior with an exponential convergence rate. It turns out that relatively simple algebraic

conditions can be given for this stability-like property to be verified, and that this property is preserved through basic system combinations.

While we shall derive global properties of nonlinear systems, many of our results can be expressed in terms of eigenvalues of symmetric matrices [14]. Given a square matrix $\mathbf{A}$, the symmetric part of $\mathbf{A}$ is denoted by $\mathbf{A}_s$. The smallest and largest eigenvalues of $\mathbf{A}_s$ are denoted by $\lambda_{\min}(\mathbf{A})$ and $\lambda_{\max}(\mathbf{A})$. Given these notations, the matrix $\mathbf{A}$ is *positive definite* (denoted $\mathbf{A} > \mathbf{0}$) if $\lambda_{\min}(\mathbf{A}) > 0$, and it is *negative definite* (denoted $\mathbf{A} < \mathbf{0}$) if $\lambda_{\max}(\mathbf{A}) < 0$. Finally, a square matrix $\mathbf{A}(\mathbf{x}, t)$ is *uniformly* positive definite if $\exists \beta > 0, \forall \mathbf{x}, \forall t : \lambda_{\min}(\mathbf{A}(\mathbf{x}, t)) \geq \beta$, and it is *uniformly* negative definite if $\exists \beta > 0, \forall \mathbf{x},\ \forall t : \lambda_{\min}(\mathbf{A}(\mathbf{x}, t)) \leq -\beta$.

The basic theorem of contraction analysis, derived in [27], can be stated as:

Theorem 1 (Contraction) *Consider, in $\mathbb{R}^n$, the deterministic system*

$$\dot{\mathbf{x}} = \mathbf{f}(\mathbf{x}, t) \tag{1}$$

where $\mathbf{f}$ is a smooth nonlinear function. Denote the Jacobian matrix of $\mathbf{f}$ with respect to its first variable by $\frac{\partial \mathbf{f}}{\partial \mathbf{x}}$. If there exists a square matrix $\mathbf{\Theta}(\mathbf{x}, t)$ such that $\mathbf{\Theta}(\mathbf{x}, t)^\top \mathbf{\Theta}(\mathbf{x}, t)$ is uniformly positive definite and the matrix

$$\mathbf{F} = \left(\dot{\mathbf{\Theta}} + \mathbf{\Theta} \frac{\partial \mathbf{f}}{\partial \mathbf{x}} \right) \mathbf{\Theta}^{-1}$$

is uniformly negative definite, then all system trajectories converge exponentially to a single trajectory, with convergence rate $|\sup_{\mathbf{x},t} \lambda_{\max}(\mathbf{F})| > 0$. The system is said to be contracting*, $\mathbf{F}$ is called its* generalized Jacobian*, and $\mathbf{\Theta}(\mathbf{x}, t)^\top \mathbf{\Theta}(\mathbf{x}, t)$ its contraction* metric*.*

It can be shown conversely that the existence of a uniformly positive definite metric $\mathbf{M}(\mathbf{x}, t) = \mathbf{\Theta}(\mathbf{x}, t)^\top \mathbf{\Theta}(\mathbf{x}, t)$ with respect to which the system is contracting is also a necessary condition for global exponential convergence of trajectories [27]. Furthermore, all transformations $\mathbf{\Theta}$ corresponding to the same $\mathbf{M}$ lead to the same eigenvalues for the symmetric part $\mathbf{F}_s$ of $\mathbf{F}$ [43], and thus to the same contraction rate $|\sup_{\mathbf{x},t} \lambda_{\max}(\mathbf{F})|$.

In the linear time-invariant case, a system is globally contracting if and only if it is strictly stable, and $\mathbf{F}$ can be chosen as a normal Jordan form of the system with $\mathbf{\Theta}$ the coordinate transformation to that form [27]. Contraction analysis can also be derived for discrete-time systems and for classes of hybrid systems [28].

Finally, it can be shown that contraction is preserved through basic system combinations (such as parallel combinations, hierarchies, and certain types of

negative feedback, see [27] for details), a property which we shall extend to the synchronization context in this paper (section 4).

Theorem 2 (Contraction and robustness) *Consider a contracting system* $\dot{\mathbf{x}} = \mathbf{f}(\mathbf{x}, t)$*, with* $\boldsymbol{\Theta} = \mathbf{I}$ *and contraction rate* λ*. Let* $P_1(t)$ *be a trajectory of the system, and let* $P_2(t)$ *be a trajectory of the* disturbed *system*

$$\dot{\mathbf{x}} = \mathbf{f}(\mathbf{x}, t) + \mathbf{d}(\mathbf{x}, t)$$

Then the distance $R(t)$ *between* $P_1(t)$ *and* $P_2(t)$ *verifies* $R(t) \leq \sup_{\mathbf{x},t} \|\mathbf{d}(\mathbf{x}, t)\|/\lambda$ *after exponential transients of rate* λ*.*

For a proof and generalisation of this theorem, see section 3.7 in [27].

2.2 Convergence to a flow-invariant subspace

We now derive a simple tool upon which the analyses of this paper will be based. The derivation is inspired by the idea of "partial" contraction, introduced in [48], which consists in applying contraction tools to virtual auxiliary systems so as to address questions more general than trajectory convergence.

Consider again, in $\mathbb{R}^n$, the deterministic system

$$\dot{\mathbf{x}} = \mathbf{f}(\mathbf{x}, t) \tag{2}$$

where $\mathbf{f}$ is a smooth nonlinear function. Assume that there exists a *flow-invariant linear subspace* $\mathcal{M}$ (i.e. a linear subspace $\mathcal{M}$ such that $\forall t : \mathbf{f}(\mathcal{M}, t) \subset \mathcal{M}$), which implies that any trajectory starting in $\mathcal{M}$ remains in $\mathcal{M}$. Let $p = \dim(\mathcal{M})$, and consider an orthonormal basis $(\mathbf{e}_1, \ldots, \mathbf{e}_n)$ where the first p vectors form a basis of $\mathcal{M}$ and the last $n - p$ a basis of $\mathcal{M}^{\perp}$. Define an $(n - p) \times n$ matrix $\mathbf{V}$ whose rows are $\mathbf{e}_{p+1}^{\top}, \ldots, \mathbf{e}_n^{\top}$. $\mathbf{V}$ may be regarded as a projection [2] on $\mathcal{M}^{\perp}$, and it verifies [14,20] :

$$\mathbf{V}^{\top}\mathbf{V} + \mathbf{U}^{\top}\mathbf{U} = \mathbf{I}_n \qquad \mathbf{V}\mathbf{V}^{\top} = \mathbf{I}_{n-p} \qquad \mathbf{x} \in \mathcal{M} \iff \mathbf{V}\mathbf{x} = \mathbf{0}$$

where $\mathbf{U}$ is the matrix formed by the first p vectors.

Theorem 3 *Consider a linear flow-invariant subspace* $\mathcal{M}$ *and the associated orthonormal projection matrix* $\mathbf{V}$*. A particular solution* $\mathbf{x}_p(t)$ *of system (2)*

[2] For simplicity we shall call $\mathbf{V}$ a "projection", although the actual projection matrix is in fact $\mathbf{V}^{\top}\mathbf{V}$.

converges exponentially to $\mathcal{M}$ *if the system*

$$\dot{\mathbf{y}} = \mathbf{V}\mathbf{f}(\mathbf{V}^\top \mathbf{y} + \mathbf{U}^\top \mathbf{U}\mathbf{x}_p(t), t) \tag{3}$$

is contracting with respect to $\mathbf{y}$.

If the above contraction condition is fullfilled for all $\mathbf{x}_p$*, then starting from any initial conditions, all trajectories of system (2) will exponentially converge to* $\mathcal{M}$*. If furthermore all the contraction rates for (3) are lower-bounded by some* $\lambda > 0$*, uniformly in* $\mathbf{x}_p$ *and in a common metric, then the convergence to* $\mathcal{M}$ *will be exponential with rate* λ *(see figure 2).*

Proof : Let $\mathbf{z}_p = \mathbf{V}\mathbf{x}_p$. By construction, $\mathbf{x}_p$ converges to the subspace $\mathcal{M}$ if and only if $\mathbf{z}_p$ converges to $\mathbf{0}$. Multiplying (2) by $\mathbf{V}$ on the left, we get

$$\dot{\mathbf{z}}_p = \mathbf{V}\mathbf{f}(\mathbf{V}^\top \mathbf{z}_p + \mathbf{U}^\top \mathbf{U}\mathbf{x}_p, t) \tag{4}$$

From (4), $\mathbf{y}(t) = \mathbf{z}_p(t)$ is a particular solution of system (3). In addition, since $\mathbf{U}^\top \mathbf{U}\mathbf{x}_p \in \mathcal{M}$ and the linear subspace $\mathcal{M}$ is flow-invariant, one has $\mathbf{f}(\mathbf{U}^\top \mathbf{U}\mathbf{x}_p) \in \mathcal{M} = \mathrm{Null}(\mathbf{V})$, and hence $\mathbf{y}(t) = \mathbf{0}$ is another particular solution of system (3). If system (3) is contracting with respect to $\mathbf{y}$, then all its solutions converge exponentially to a single trajectory, which implies in particular that $\mathbf{z}_p(t)$ converges exponentially to $\mathbf{0}$.

The remainder of the theorem is immediate. □

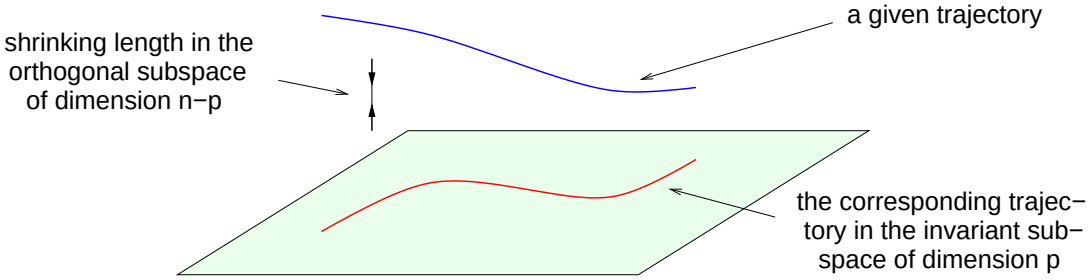

Fig. 2. Convergence to a linear flow-invariant subspace

Corollary 1 *A simple sufficient condition for global exponential convergence to* $\mathcal{M}$ *is that*

$$\mathbf{V}\frac{\partial \mathbf{f}}{\partial \mathbf{x}}\mathbf{V}^\top < \mathbf{0} \quad \text{uniformly} \tag{5}$$

or more generally, that there exists a constant invertible transform $\mathbf{\Theta}$ *on* $\mathcal{M}^\perp$ *such that*

$$\mathbf{\Theta}\mathbf{V}\frac{\partial \mathbf{f}}{\partial \mathbf{x}}\mathbf{V}^\top\mathbf{\Theta}^{-1} < \mathbf{0} \quad \text{uniformly} \tag{6}$$

Proof : The Jacobian of (3) with respect to $\mathbf{y}$ is

$$\mathbf{V}\left[\frac{\partial \mathbf{f}}{\partial \mathbf{x}}\left(\mathbf{V}^\top \mathbf{y} + \mathbf{U}^\top \mathbf{U}\mathbf{x}_p(t), t\right)\right]\mathbf{V}^\top$$

so that the result is immediate by applying Theorem 1. □

Remarks

- *Non-orthonormal bases.* In practice, the subspace $\mathcal{M}$ is often defined by the conjunction of $(n-p)$ linear constraints. In a synchronization context, for instance, each of the constraints may be, e.g., of the form $\mathbf{x}_i = \mathbf{x}_j$ where $\mathbf{x}_i$ and $\mathbf{x}_j$ are subvectors of the state $\mathbf{x}$. This provides directly a (generally not orthonormal) basis $(\mathbf{e}'_{p+1}, \ldots, \mathbf{e}'_n)$ of $\mathcal{M}^\perp$, and thus a matrix $\mathbf{V}'$ whose rows are ${\mathbf{e}'_{p+1}}^\top, \ldots, {\mathbf{e}'_n}^\top$, and which verifies

  $$\mathbf{V}' = \mathbf{T}\mathbf{V}$$

  with $\mathbf{T}$ an invertible $(n-p)\times(n-p)$ matrix. We have $\mathbf{x} \in \mathcal{M} \iff \mathbf{V}'\mathbf{x} = \mathbf{0}$ and

  $$\mathbf{V}\frac{\partial \mathbf{f}}{\partial \mathbf{x}}\mathbf{V}^\top < \mathbf{0} \iff \mathbf{V}'\frac{\partial \mathbf{f}}{\partial \mathbf{x}}{\mathbf{V}'}^\top < \mathbf{0} \tag{7}$$

  Consider for instance three systems of dimension m and two systems of dimension p, and assume that $\mathcal{M} = \{\mathbf{x}_1 = \mathbf{x}_2, \mathbf{x}_5 = -10\mathbf{x}_4\}$ is the synchronization subspace of interest (with $\mathbf{x}_i$ denoting the state of each individual system). One has directly

  $$\mathbf{V}' = \begin{pmatrix} \mathbf{I}_m & -\mathbf{I}_m & \mathbf{0} & \cdots & \mathbf{0} \\ \mathbf{0} & \cdots & \mathbf{0} & 10\mathbf{I}_p & \mathbf{I}_p \end{pmatrix}$$

  Note however that the equivalence in equation (7) does not yield the same upper bound for the eigenvalues of the two matrices. Thus, in order to compute explicitly the convergence rate to $\mathcal{M}$, one has to revert to the orthonormal version, using e.g. a Gram-Schmidt procedure [14] on the rows of $\mathbf{V}'$.
- *More general invariant subspaces.* This theorem can be extended straightforwardly to time-varying affine invariant subspaces of the form $\mathbf{m}(t) + \mathcal{M}$ (apply the theorem to $\tilde{\mathbf{x}}(t) = \mathbf{x}(t) - \mathbf{m}(t)$). Preliminary results have also been obtained for nonlinear invariant manifolds [35].

2.3 Global synchronization in networks of coupled identical dynamical elements

In this section, we provide by using theorem 3 a unifying and systematic view on several prior results in the study of synchronization phenomena (see e.g. [19,36,48,33,26] and references therein).

Consider first a network containing n identical dynamical elements with *diffusive* couplings [48]

$$\dot{\mathbf{x}}_i = \mathbf{f}(\mathbf{x}_i, t) + \sum_{j \neq i} \mathbf{K}_{ij}(\mathbf{x}_j - \mathbf{x}_i) \qquad i = 1, \ldots, n \tag{8}$$

Let $\mathbf{L}$ be the Laplacian matrix of the network ($\mathbf{L}_{ii} = \sum_{j \neq i} \mathbf{K}_{ij}$, $\mathbf{L}_{ij} = -\mathbf{K}_{ij}$ for $j \neq i$), and [3]

$$\widehat{\mathbf{x}} = \begin{pmatrix} \mathbf{x}_1 \\ \vdots \\ \mathbf{x}_n \end{pmatrix}, \quad \widehat{\mathbf{f}}(\widehat{\mathbf{x}}, t) = \begin{pmatrix} \mathbf{f}(\mathbf{x}_1, t) \\ \vdots \\ \mathbf{f}(\mathbf{x}_n, t) \end{pmatrix}$$

Equation (8) can be rewritten in matrix form

$$\dot{\widehat{\mathbf{x}}} = \widehat{\mathbf{f}}(\widehat{\mathbf{x}}, t) - \mathbf{L}\widehat{\mathbf{x}} \tag{9}$$

The Jacobian matrix of this system is $\mathbf{J} = \widehat{\mathbf{G}} - \mathbf{L}$, where

$$\widehat{\mathbf{G}}(\widehat{\mathbf{x}}, t) = \begin{pmatrix} \frac{\partial \mathbf{f}}{\partial \mathbf{x}}(\mathbf{x}_1, t) & \mathbf{0} & \mathbf{0} \\ \mathbf{0} & \ddots & \mathbf{0} \\ \mathbf{0} & \mathbf{0} & \frac{\partial \mathbf{f}}{\partial \mathbf{x}}(\mathbf{x}_n, t) \end{pmatrix}$$

Let now $(\mathbf{e}_1, \ldots, \mathbf{e}_d)$ be a basis of the state space of one element and consider the following vectors of the global state space

$$\widehat{\mathbf{e}}_1 = \begin{pmatrix} \mathbf{e}_1 \\ \vdots \\ \mathbf{e}_1 \end{pmatrix}, \ldots, \widehat{\mathbf{e}}_d = \begin{pmatrix} \mathbf{e}_d \\ \vdots \\ \mathbf{e}_d \end{pmatrix},$$

[3] The overscript $\frown$ denotes a vector in the global state space, obtained by grouping together the states of the elements.

Let $\mathcal{M} = \text{span}\{\widehat{\mathbf{e}}_1, \ldots, \widehat{\mathbf{e}}_d\}$ be the "diagonal" subspace spanned by the $\widehat{\mathbf{e}}_i$. Note that $\widehat{\mathbf{x}}^* \in \mathcal{M}$ if and only if $\mathbf{x}_1^* = \ldots = \mathbf{x}_n^*$, i.e. all elements are in synchrony. In such a case, all coupling forces equal zero, and the individual dynamics are the same for every element. Hence

$$\widehat{\mathbf{f}}(\widehat{\mathbf{x}}^*, t) - \mathbf{L}\widehat{\mathbf{x}}^* = \begin{pmatrix} \mathbf{f}(\mathbf{x}_1^*, t) \\ \vdots \\ \mathbf{f}(\mathbf{x}_1^*, t) \end{pmatrix} \in \mathcal{M}$$

which means that $\mathcal{M}$ is flow-invariant.

Consider, as in section 2.2, the projection matrix $\mathbf{V}$ on $\mathcal{M}^\perp$. Since $\mathbf{V}$ is built from orthonormal vectors, $\lambda_{\max}(\mathbf{V}\widehat{\mathbf{G}}(\widehat{\mathbf{x}}, t)\mathbf{V}^\top)$ is upper-bounded by $\max_i \lambda_{\max}\left(\frac{\partial \mathbf{f}}{\partial \mathbf{x}}(\mathbf{x}_i, t)\right)$. Thus, by virtue of theorem 3, a simple sufficient condition for global exponential synchronization is

$$\lambda_{\min}(\mathbf{V}\mathbf{L}\mathbf{V}^\top) \; > \; \sup_{\mathbf{a},t} \lambda_{\max}\left(\frac{\partial \mathbf{f}}{\partial \mathbf{x}}(\mathbf{a}, t)\right) \tag{10}$$

Furthermore, the *synchronization rate*, i.e. the rate of convergence to the synchronization subspace, is the *contraction rate* of the auxiliary system (3).

Let us now make some brief remarks.

- **(i)** *Undirected* [4] *diffusive networks.* In this case, it is well known that $\mathbf{L}$ is symmetric positive semi-definite, and that $\mathcal{M}$ is a subset of the eigenspace corresponding to the eigenvalue 0 [7]. Furthermore, if the network is *connected*, this eigenspace is exactly $\mathcal{M}$, and therefore $\mathbf{V}\mathbf{L}\mathbf{V}^\top$ is positive definite (its smallest eigenvalue is called the network's *algebraic connectivity* [7]). Assume now that $\mathbf{L}$ is parameterized by a positive scalar k (i.e. $\mathbf{L} = k\mathbf{L}_0$, for some $\mathbf{L}_0$), and that $\frac{\partial \mathbf{f}}{\partial \mathbf{x}}$ is upper-bounded. Then, for large enough k (i.e. for strong enough coupling strength), all elements will synchronize exponentially.
- **(ii)** *Network of contracting elements.* If the elements $\mathbf{x}_i$ are already *contracting* when taken in isolation (i.e. $\frac{\partial \mathbf{f}}{\partial \mathbf{x}}$ is uniformly negative definite), then in presence of *weak or non-existent couplings* ($\mathbf{V}\mathbf{L}\mathbf{V}^\top = 0$), the Jacobian matrix $\mathbf{J}$ of the global system will remain uniformly negative definite [48]. Thus, the projected Jacobian matrix will be *a fortiori* uniformly negative definite, implying exponential convergence to the synchronized state.

[4] "Undirected" is to be understood here in the graph-theoretical sense, i.e. : for all i, j, the connection from i to j is the same as the one from j to i. Therefore, an undirected network can be represented by an undirected graph, where each edge stands for two connections, one in each direction.

One can also obtain this conclusion by using a "pure" contraction analysis. Indeed, choose a particular initial state where $\mathbf{x}_1(0) = \ldots = \mathbf{x}_n(0)$. The trajectory starting with that initial state verifies $\forall t, \mathbf{x}_1(t) = \ldots = \mathbf{x}_n(t)$ by flow-invariance. Since the global system is contracting, any other initial conditions will lead exponentially to that particular trajectory, i.e., starting with any initial conditions, the system will exponentially converge to a synchronized state.

(iii) *Nonlinear couplings.* Similarly to [48], the above result actually extends to nonlinear couplings described by a Laplacian matrix $\mathbf{L}(\widehat{\mathbf{x}}, t)$. Replacing the auxiliary system (3) by

$$\dot{\mathbf{y}} = \mathbf{V}\widehat{\mathbf{f}}(\mathbf{V}^\top \mathbf{y} + \mathbf{U}^\top \mathbf{U}\widehat{\mathbf{x}}_p, t) - \mathbf{V}\mathbf{L}(\widehat{\mathbf{x}}_p, t)(\mathbf{V}^\top \mathbf{y} + \mathbf{U}^\top \mathbf{U}\widehat{\mathbf{x}}_p)$$

the same steps show that global synchronization is achieved exponentially for

$$\inf_{\widehat{\mathbf{x}},t} \lambda_{\min}(\mathbf{V}\mathbf{L}(\widehat{\mathbf{x}}, t)\mathbf{V}^\top) \; > \; \sup_{\mathbf{a},t} \lambda_{\max}\left(\frac{\partial \mathbf{f}}{\partial \mathbf{x}}(\mathbf{a}, t)\right)$$

(iv) *Leader-followers network.* Assume that there exists a *leader* $\mathbf{x}_\ell$ in the network [48], i.e., an element which has no *incoming* connections from the other elements, $\dot{\mathbf{x}}_\ell = \mathbf{f}(\mathbf{x}_\ell, t)$. Convergence to $\mathcal{M}$ (guaranteed by satisfying (10)) then implies that all the network elements will synchronize to the leader trajectory $\mathbf{x}_\ell(t)$.

(v) *Non-diffusive couplings.* Note that the above results are actually not limited to diffusive couplings but apply to any system of the general form (9). This point will be further illustrated in sections 3.1 and 3.2.

3 Main discussion

In nonlinear contraction theory, the analysis of dynamical systems is greatly simplified by studying stability and nominal motion separately. We propose a similar point of view for analyzing synchronization in networks of dynamical systems. In section 3.1, we study specific conditions on the coupling structure which guarantee exponential convergence to a linear subspace. In section 3.2, we examine how symmetries and/or diffusion-like couplings can give rise to specific flow-invariant subspaces corresponding to concurrent synchronized states.

3.1.1 Balanced diffusive networks

A balanced network [33] is a directed diffusive network which verifies the following equality for each node i (see figure 3 for an example)

$$\sum_{j\neq i} \mathbf{K}_{ij} = \sum_{j\neq i} \mathbf{K}_{ji}$$

Because of this property, the symmetric part of the Laplacian matrix of the network is itself the Laplacian matrix of the underlying undirected graph to the network [5] . Thus, the positive definiteness of $\mathbf{VLV}^\top$ for a balanced network is equivalent to the connectedness of some well-defined undirected graph.

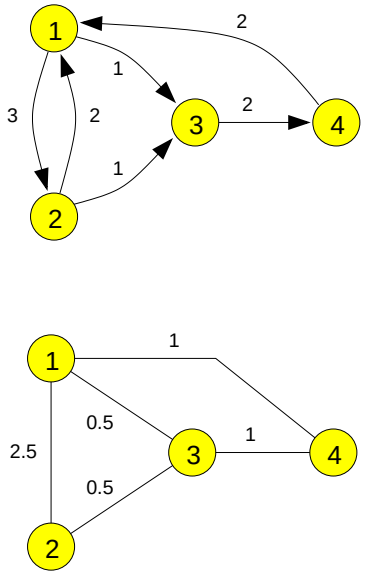

Fig. 3. A balanced network with Laplacian matrix

$$\mathbf{L} = \begin{pmatrix} 4 & -2 & 0 & -2 \\ -3 & 3 & 0 & 0 \\ -1 & -1 & 2 & 0 \\ 0 & 0 & -2 & 2 \end{pmatrix}$$

Its underlying undirected graph, with Laplacian matrix

$$\mathbf{L}_s = \tfrac{\mathbf{L}+\mathbf{L}^\top}{2} = \begin{pmatrix} 4 & -2.5 & -0.5 & -1 \\ -2.5 & 3 & -0.5 & 0 \\ -0.5 & -0.5 & 2 & -1 \\ -1 & 0 & -1 & 2 \end{pmatrix}$$

For general directed diffusive networks, finding a simple condition implying the positive definiteness of $\mathbf{VLV}^\top$ (such as the connectivity condition in the case of undirected networks) still remains an open problem. However, given a particular example, one can compute $\mathbf{VLV}^\top$ and determine directly whether it is positive definite.

[5] In fact, it is easy to see that the symmetric part of the Laplacian matrix of a directed graph is the Laplacian matrix of some undirected graph *if and only if* the directed graph is balanced.

3.1.2 Extension of diffusive connections

In some applications [49], one might encounter the following dynamics

$$\begin{cases} \dot{\mathbf{x}}_1 = \mathbf{f}_1(\mathbf{x}_1, t) + k\mathbf{A}^\top(\mathbf{B}\mathbf{x}_2 - \mathbf{A}\mathbf{x}_1) \\ \dot{\mathbf{x}}_2 = \mathbf{f}_2(\mathbf{x}_2, t) + k\mathbf{B}^\top(\mathbf{A}\mathbf{x}_1 - \mathbf{B}\mathbf{x}_2) \end{cases}$$

Here $\mathbf{x}_1$ and $\mathbf{x}_2$ can be of different dimensions, say d_1 and d_2. $\mathbf{A}$ and $\mathbf{B}$ are constant matrices of appropriate dimensions. The Jacobian matrix of the overall system is

$$\mathbf{J} = \begin{pmatrix} \frac{\partial \mathbf{f}_1}{\partial \mathbf{x}_1} & \\ & \frac{\partial \mathbf{f}_2}{\partial \mathbf{x}_2} \end{pmatrix} - k\mathbf{L}, \quad \text{where } \mathbf{L} = \begin{pmatrix} \mathbf{A}^\top\mathbf{A} & -\mathbf{A}^\top\mathbf{B} \\ -\mathbf{B}^\top\mathbf{A} & \mathbf{B}^\top\mathbf{B} \end{pmatrix}$$

Note that $\mathbf{L}$ is symmetric positive semi-definite. Indeed, one immediately verifies that

$$\forall \mathbf{x}_1, \mathbf{x}_2 : \begin{pmatrix} \mathbf{x}_1 & \mathbf{x}_2 \end{pmatrix} \mathbf{L} \begin{pmatrix} \mathbf{x}_1 \\ \mathbf{x}_2 \end{pmatrix} = (\mathbf{A}\mathbf{x}_1 - \mathbf{B}\mathbf{x}_2)^\top(\mathbf{A}\mathbf{x}_1 - \mathbf{B}\mathbf{x}_2) \geq 0$$

Consider now the linear subspace of $\mathbb{R}^{d_1} \times \mathbb{R}^{d_2}$ defined by

$$\mathcal{M} = \left\{ \begin{pmatrix} \mathbf{x}_1 \\ \mathbf{x}_2 \end{pmatrix} \in \mathbb{R}^{d_1} \times \mathbb{R}^{d_2} : \mathbf{A}\mathbf{x}_1 - \mathbf{B}\mathbf{x}_2 = \mathbf{0} \right\}$$

and use as before the orthonormal projection $\mathbf{V}$ on $\mathcal{M}^\perp$, so that $\mathbf{V}\mathbf{L}\mathbf{V}^\top$ is positive definite. Assume furthermore that $\mathcal{M}$ is flow-invariant, i.e.

$$\forall (\mathbf{x}_1, \mathbf{x}_2) \in \mathbb{R}^{d_1} \times \mathbb{R}^{d_2}, [\mathbf{A}\mathbf{x}_1 = \mathbf{B}\mathbf{x}_2] \Rightarrow [\mathbf{A}\mathbf{f}_1(\mathbf{x}_1) = \mathbf{B}\mathbf{f}_2(\mathbf{x}_2)]$$

and that the Jacobian matrices of the individual dynamics are upper-bounded. Then large enough k, i.e. for example

$$k\lambda_{\min}(\mathbf{V}\mathbf{L}\mathbf{V}^\top) > \max_{i=1,2} \left(\sup_{\mathbf{a}_i, t} \lambda_{\max} \frac{\partial \mathbf{f}_i}{\partial \mathbf{x}_i}(\mathbf{a}_i, t) \right)$$

ensures exponential convergence to the subspace $\mathcal{M}$.

The state corresponding to $\mathcal{M}$ can be viewed as an extension of synchronization states to systems of different dimensions. Indeed, in the case where $\mathbf{x}_1$

and $\mathbf{x}_2$ have the same dimension and where $\mathbf{A} = \mathbf{B}$ are non singular, we are in the presence of classical diffusive connections, which leads us back to the discussion of section 2.3.

As in the case of diffusive connections, one can consider networks of so-connected elements, for example :

$$\begin{cases} \dot{\mathbf{x}}_1 = \mathbf{f}_1(\mathbf{x}_1, t) + \mathbf{A}_B^\top(\mathbf{B}_A\mathbf{x}_2 - \mathbf{A}_B\mathbf{x}_1) + \mathbf{A}_C^\top(\mathbf{C}_A\mathbf{x}_3 - \mathbf{A}_C\mathbf{x}_1) \\ \dot{\mathbf{x}}_2 = \mathbf{f}_2(\mathbf{x}_2, t) + \mathbf{B}_C^\top(\mathbf{C}_B\mathbf{x}_3 - \mathbf{B}_C\mathbf{x}_2) + \mathbf{B}_A^\top(\mathbf{A}_B\mathbf{x}_1 - \mathbf{B}_A\mathbf{x}_2) \\ \dot{\mathbf{x}}_3 = \mathbf{f}_3(\mathbf{x}_2, t) + \mathbf{C}_A^\top(\mathbf{A}_C\mathbf{x}_1 - \mathbf{C}_A\mathbf{x}_3) + \mathbf{C}_B^\top(\mathbf{B}_C\mathbf{x}_2 - \mathbf{C}_B\mathbf{x}_3) \end{cases}$$

leads to a positive semi-definite Laplacian matrix

$$\begin{pmatrix} \mathbf{A}_B^\top\mathbf{A}_B & -\mathbf{A}_B^\top\mathbf{B}_A & \mathbf{0} \\ -\mathbf{B}_A^\top\mathbf{A}_B & \mathbf{B}_A^\top\mathbf{B}_A & \mathbf{0} \\ \mathbf{0} & \mathbf{0} & \mathbf{0} \end{pmatrix} + \begin{pmatrix} \mathbf{0} & \mathbf{0} & \mathbf{0} \\ \mathbf{0} & \mathbf{B}_C^\top\mathbf{B}_C & -\mathbf{B}_C^\top\mathbf{C}_B \\ \mathbf{0} & -\mathbf{C}_B^\top\mathbf{B}_C & \mathbf{C}_B^\top\mathbf{C}_B \end{pmatrix} + \begin{pmatrix} \mathbf{A}_C^\top\mathbf{A}_C & \mathbf{0} & -\mathbf{A}_C^\top\mathbf{C}_A \\ \mathbf{0} & \mathbf{0} & \mathbf{0} \\ -\mathbf{C}_A^\top\mathbf{A}_C & \mathbf{0} & \mathbf{C}_A^\top\mathbf{C}_A \end{pmatrix}$$

and potentially a flow-invariant subspace

$$\mathcal{M} = \{\mathbf{A}_B\mathbf{x}_1 = \mathbf{B}_A\mathbf{x}_2\} \cap \{\mathbf{B}_C\mathbf{x}_2 = \mathbf{C}_B\mathbf{x}_3\} \cap \{\mathbf{C}_A\mathbf{x}_3 = \mathbf{A}_C\mathbf{x}_1\}$$

The above coupling structures can be implemented in nonlinear versions of the predictive hierarchies used in image processing (e.g. [29,5,37,24,10,38]).

3.1.3 Excitatory-only networks

One can also address the case of networks with excitatory-only connections. Consider for instance the following system and its Jacobian matrix [6]

$$\begin{cases} \dot{x}_1 = f(x_1, t) + kx_2 \\ \dot{x}_2 = f(x_2, t) + kx_1 \end{cases} \qquad \mathbf{J} = \begin{pmatrix} \frac{\partial f}{\partial x}(x_1, t) & 0 \\ 0 & \frac{\partial f}{\partial x}(x_2, t) \end{pmatrix} + k \begin{pmatrix} 0 & 1 \\ 1 & 0 \end{pmatrix}$$

Clearly, $\mathrm{span}\{(1,1)\}$ is flow-invariant. Applying the methodology described above, we choose $\mathbf{V} = \frac{1}{\sqrt{2}}(1,-1)$, so that the projected Jacobian matrix is

[6] For the sake of clarity, the elements are assumed to be 1-dimensional. However, the same reasoning applies for the multidimensional case as well: instead of $\mathrm{span}\left\{\begin{pmatrix} 1 \\ 1 \end{pmatrix}\right\}$, one considers $\mathrm{span}\{\widehat{\mathbf{e}}_1, \ldots, \widehat{\mathbf{e}}_d\}$ as in section 2.3.

$\frac{1}{2}\left(\frac{\partial f}{\partial x}(x_1,t)+\frac{\partial f}{\partial x}(x_2,t)\right)-k$. Thus, for $k > \sup_{a,t}\frac{\partial f}{\partial x}(a,t)$, the two elements synchronize exponentially.

In the case of diffusive connections, once the elements are synchronized, the coupling terms disappear, so that each individual element exhibits its natural, uncoupled behavior. This is not the case with excitatory-only connections. This is illustrated in figure 4 using FitzHugh-Nagumo oscillator models (see appendix A for the contraction analysis of coupled FitzHugh-Nagumo oscillators).

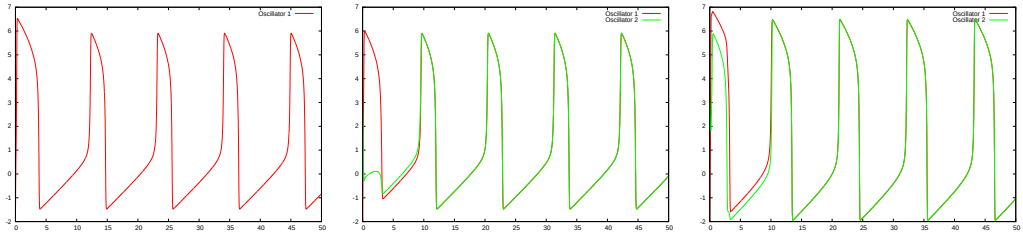

Fig. 4. From left to right : a single oscillator, two oscillators coupled through diffusive connections, two oscillators coupled through excitatory-only connections.

3.1.4 Rate models for neuronal populations

In computational neuroscience, one often uses the following simplified equations to model the dynamics of neuronal populations

$$\tau\dot{\mathbf{x}}_i = -\mathbf{x}_i + \Phi\left(\sum_{j\neq i} k_{ij}\mathbf{x}_j(t)\right) + \mathbf{u}_i(t)$$

Assume that the external inputs $\mathbf{u}_i(t)$ are all equal, and that the synaptic connections k_{ij} verify $\exists c, \forall i,\ \sum_{j\neq i} k_{ij} = c$ (i.e., that they induce input-equivalence, see section 3.2). Then the synchronization subspace $\{\mathbf{x}_1 = \ldots = \mathbf{x}_n\}$ is flow-invariant. Furthermore, since each element, taken in isolation, is *contracting* with contraction rate $1/\tau$, synchronization should occur when the coupling is not too strong (see remark (ii) in section 2.3).

Specifically, consider first the case where Φ is a linear function : $\Phi(\mathbf{x}) = \mu\mathbf{x}$. The Jacobian matrix of the global system is then $-\mathbf{I}_n + \mu\mathbf{K}$, where $\mathbf{K}$ is the matrix of k_{ij}. Using the result of remark (ii) in section 2.3, a sufficient condition for the system to be contracting (and thus synchronizing) is that the couplings are *weak* enough (or more precisely, such that $\mu\lambda_{\max}(\mathbf{K}) < 1$).

The same condition is obtained if Φ is now e.g. a multidimentional *sigmoid* of maximum slope μ (see remark (iii) in section 2.3).

Besides the synchronization behavior of these models, their natural *contraction* property for weak enough couplings of any sign is interesting in its own right. Indeed, given a set of (not necessarily equal) external inputs $\mathbf{u}_i(t)$, all trajectories of the global system will converge to a unique trajectory, independently of initial conditions.

3.2 Symmetries, diffusion-like couplings, flow-invariant subspaces and concurrent synchronization

Synchronized states can be created in at least two ways : by architectural and internal [7] symmetries [11,12,6,36] or by diffusion-like couplings [48,20,33,26,2]. Actually, we shall see that both, together or separately, can create flow-invariant subspaces corresponding to concurrently synchronized states.

3.2.1 Symmetries and input-equivalence

In section 2.3, we argued that, in the case of coupled *identical* elements, the global synchronization subspace $\mathcal{M}$ represents a flow-invariant linear subspace of the global state space. However, several previous works have pointed out that larger (less restrictive) flow-invariant subspaces may exist if the network exhibits symmetries [52,2,36], even when the systems are *not* identical [11].

The main idea behind these works can be summarized as follows. Assume that the network is divided into k aspiring synchronized groups $S_1, \ldots, S_k$ [8]. The flow-invariant subspace corresponding to this regime (in the sequel, we shall call such a subspace a *concurrent synchronization subspace*), namely

$$\{(\mathbf{x}_1; \ldots; \mathbf{x}_n) : \forall 1 \leq m \leq k, \forall i, j \in S_m : \mathbf{x}_i = \mathbf{x}_j\}$$

is flow-invariant if, for each S_m, the following conditions are true :

(i) if $i, j \in S_m$, then they have a same individual (uncoupled) dynamics
(ii) if $i, j \in S_m$, and if they receive their input from elements i' and j' respectively, then i' and j' must be in a same group $S_{m'}$, and the coupling functions $i' \to i$ and $j' \to j$ must be identical (i.e., the connections must have identical dynamics and/or delays). If i and j have more than one

[7] Internal symmetries can easily be analyzed within our framework as leading to flow-invariant subspaces, and we shall use this property in section 5.3 for building central pattern generators. However, they will not be discussed in detail in this article. The interested reader can consult [6].
[8] Some groups may contain a single element, see section 4.2.3.

input, they must have the same number of inputs, and the above conditions must be true for each input. In this case, we say that i and j are input-symmetric, or more precisely, *input-equivalent* (since formally "symmetry" implies the action of a group).

One can see here that symmetry, or more generally input-equivalence, plays a key role in concurrent synchronization. For a more detailed discussion, the reader is referred to [11,12].

Remark : One can thus turn on/off a specific symmetry by turning on/off a single connection. This has similarities to the fact that a single inhibitory connection can turn on/off an entire network of synchronized identical oscillators [48].

3.2.2 Diffusion-like couplings

The condition of input-equivalence can be relaxed when some connections *within a group* are null when the connected elements are in the same state. Such connections are pervasive in the literature : diffusive connections (in a neuronal context, they correspond to electrical synapses mediated by gap junctions [41,9], in an automatic control context, they correspond to poursuit or velocity matching strategies [33,26], ...), connections in the Kuramoto model [18,20,45] (i.e. in the form $\dot{x_i} = f(x_i, t) + \sum_j k_{ij} \sin(x_j - x_i)$), etc.

Indeed, consider for instance diffusive connections and assume that

- $i, i', j, j' \in S_m$
- $i' \to i$ has the form $\mathbf{K}_1(\mathbf{x}_{i'} - \mathbf{x}_i)$
- $j' \to j$ has the form $\mathbf{K}_2(\mathbf{x}_{j'} - \mathbf{x}_j)$ with possibly $\mathbf{K}_1 \neq \mathbf{K}_2$

Here, i and j are not input-equivalent in the sense we defined above, but the subspace $\{\mathbf{x}_i = \mathbf{x}_j = \mathbf{x}_{i'} = \mathbf{x}_{j'}\}$ is still flow-invariant. Indeed, once the system is on this synchronization subspace, we have $\mathbf{x}_i = \mathbf{x}_{i'}$, $\mathbf{x}_j = \mathbf{x}_{j'}$, so that the diffusive couplings $i' \to i$ and $j' \to j$ vanish.

One can also view the network as a directed graph G, where the elements are represented by nodes, and connections $i \to j$ by directed arcs $i \to j$. Then, the above remark can be reformulated as

1 : for all m, color the nodes of S_m with a color m,
2 : for all m, erase the arcs representing diffusion-like connections and joining two nodes in S_m,
3 : check whether the initial coloring is balanced (in the sense of [11]) with respect to the so-obtained graph.

It should be clear by now that our framework is particularly suited to analyze concurrent synchronization. Indeed, a general methodology to show global exponential convergence to a concurrent synchronization regime consists in the following two steps

- First, find an flow-invariant linear subspace by taking advantage of potential symmetries in the network and/or diffusion-like connections.
- Second, compute the projected Jacobian matrix on the orthogonal subspace and show that it is uniformly negative definite (by explicitly computing its eigenvalues or by using results regarding the form of the network, e.g. remark (i) in section 2.3 or section 3.1).

3.3 Illustrative examples

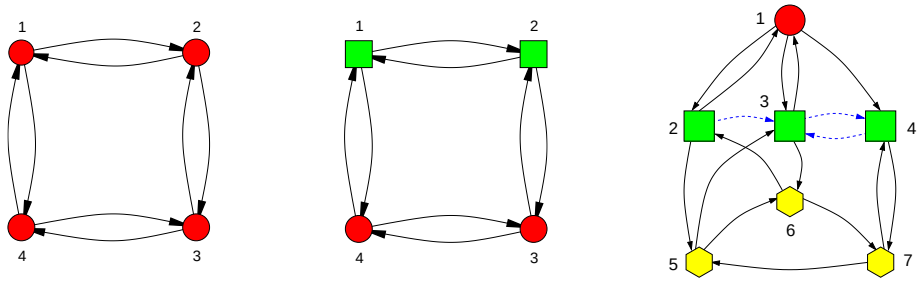

Fig. 5. Three example networks

(i) The first network has three non-trivial flow-invariant subspaces other than the global sync subspace, namely $\mathcal{M}_1 = \{\mathbf{x}_1 = \mathbf{x}_2, \mathbf{x}_3 = \mathbf{x}_4\}$, $\mathcal{M}_2 = \{\mathbf{x}_1 = \mathbf{x}_3, \mathbf{x}_2 = \mathbf{x}_4\}$, and $\mathcal{M}_3 = \{\mathbf{x}_1 = \mathbf{x}_4, \mathbf{x}_2 = \mathbf{x}_3\}$. Any of these subspaces is a strict superset of the global sync subspace, and therefore one should expect that the convergence to any of the concurrent sync state is "easier" than the convergence to the global sync state [52,2,36]. This can be quantified from (10), by noticing that

$$\mathcal{M}_A \supset \mathcal{M}_B \Rightarrow \mathcal{M}_A^{\perp} \subset \mathcal{M}_B^{\perp} \Rightarrow \lambda_{\min}(\mathbf{V}_A \mathbf{L} \mathbf{V}_A^{\top}) \geq \lambda_{\min}(\mathbf{V}_B \mathbf{L} \mathbf{V}_B^{\top}) \quad (11)$$

While in the case of identical systems and relatively uniform topologies, this "percolation" effect may often be too fast to observe, (11) applies to the general concurrent synchronization case and quantifies the associated and possibly very distinct time-scales.

(ii) The second network has only one non-trivial flow-invariant subspace $\{\mathbf{x}_1 = \mathbf{x}_2, \mathbf{x}_3 = \mathbf{x}_4\}$.

(iii) If the dashed blue arrows represent diffusive connections then the third network will have one non-trivial flow-invariant subspace $\{\mathbf{x}_2 = \mathbf{x}_3 = \mathbf{x}_4, \mathbf{x}_5 = \mathbf{x}_6 = \mathbf{x}_7\}$, even if these extra diffusive connections *obviously break the symmetry.*

Let's study in more detail this third network, in which the connections between the round element and the square ones are modelled by trigonometric functions (we shall see in section 4.2.3 that their exact form has no actual influence on the convergence rate).

$$\begin{cases} \dot{v}_1 = f(v_1) + a_1\cos(v_2) + a_2\sin(v_3) \\ \dot{v}_2 = g(v_2) + a_4\sin(v_1) + c_1 v_6 \\ \dot{v}_3 = g(v_3) + a_4\sin(v_1) + b_1(v_2 - v_3) + b_2(v_4 - v_3) + c_1 v_5 \\ \dot{v}_4 = g(v_4) + a_4\sin(v_1) + b_3(v_3 - v_4) + c_1 v_7 \\ \dot{v}_5 = h(v_5) + c_2 v_2 + (d_2 v_7 - d_1 v_5) \\ \dot{v}_6 = h(v_6) + c_2 v_3 + (d_2 v_5 - d_1 v_6) \\ \dot{v}_7 = h(v_7) + c_2 v_4 + (d_2 v_6 - d_1 v_7) \end{cases}$$

The Jacobian matrix of the couplings is

$$\mathbf{L} = \begin{pmatrix} 0 & a_1\sin(v_2) & -a_2\cos(v_3) & 0 & 0 & 0 & 0 \\ -a_4\cos(v_1) & 0 & 0 & 0 & 0 & -c_1 & 0 \\ -a_4\cos(v_1) & -b_1 & b_1 + b_2 & -b_2 & -c_1 & 0 & 0 \\ -a_4\cos(v_1) & 0 & -b_3 & b_3 & 0 & 0 & -c_1 \\ 0 & -c_2 & 0 & 0 & d_1 & 0 & -d_2 \\ 0 & 0 & -c_2 & 0 & -d_2 & d_1 & 0 \\ 0 & 0 & 0 & -c_2 & 0 & -d_2 & d_1 \end{pmatrix}$$

As we remarked previously, the concurrent synchronization regime $\{v_2 = v_3 = v_4, v_5 = v_6 = v_7\}$ is possible. Bases of the linear subspaces $\mathcal{M}$ and $\mathcal{M}^\perp$ corresponding to this regime are

$$\begin{pmatrix} 1 \\ 0 \\ 0 \\ 0 \\ 0 \\ 0 \\ 0 \end{pmatrix}, \begin{pmatrix} 0 \\ 1 \\ 1 \\ 1 \\ 0 \\ 0 \\ 0 \end{pmatrix}, \begin{pmatrix} 0 \\ 0 \\ 0 \\ 0 \\ 1 \\ 1 \\ 1 \end{pmatrix} \quad \text{for } \mathcal{M}, \text{ and} \quad \begin{pmatrix} 0 \\ \frac{\sqrt{6}}{3} \\ \frac{-\sqrt{6}}{6} \\ \frac{-\sqrt{6}}{6} \\ 0 \\ 0 \\ 0 \end{pmatrix}, \begin{pmatrix} 0 \\ 0 \\ \frac{-\sqrt{2}}{2} \\ \frac{\sqrt{2}}{2} \\ 0 \\ 0 \\ 0 \end{pmatrix}, \begin{pmatrix} 0 \\ 0 \\ 0 \\ 0 \\ \frac{\sqrt{6}}{3} \\ \frac{-\sqrt{6}}{6} \\ \frac{-\sqrt{6}}{6} \end{pmatrix}, \begin{pmatrix} 0 \\ 0 \\ 0 \\ 0 \\ 0 \\ \frac{-\sqrt{2}}{2} \\ \frac{\sqrt{2}}{2} \end{pmatrix} \quad \text{for } \mathcal{M}^\perp.$$

Group together the vectors of the basis of $\mathcal{M}^{\perp}$ into a matrix $\mathbf{V}$ and compute

$$\mathbf{V}\mathbf{L}_s\mathbf{V}^{\top} = \begin{pmatrix} \frac{b_1}{2} & -\frac{\sqrt{3}(2b_1+b_2-b_3)}{6} & \frac{c_1-2c_2}{4} & -\frac{c_1\sqrt{3}}{4} \\ -\frac{\sqrt{3}(2b_1+b_2-b_3)}{6} & \frac{b_1+2(b_2+b_3)}{2} & -\frac{c_1\sqrt{3}}{4} & -\frac{c_1+2c_2}{4} \\ \frac{c_1-2c_2}{4} & -\frac{c_1\sqrt{3}}{4} & \frac{2d_1+d_2}{2} & 0 \\ -\frac{c_1\sqrt{3}}{4} & -\frac{c_1+2c_2}{4} & 0 & \frac{2d_1+d_2}{2} \end{pmatrix}$$

As a numerical example, let $b_1 = 3\alpha$, $b_2 = 4\alpha$, $b_3 = 5\alpha$, $c_1 = \alpha$, $c_2 = 2\alpha$, $d_1 = 3\alpha$, $d_2 = 4\alpha$ and evaluate the eigenvalues of $\mathbf{V}\mathbf{L}_s\mathbf{V}^{\top}$. We obtain approximately 1.0077α for the smallest eigenvalue. Using again FitzHugh-Nagumo oscillators and based on their contraction analysis in appendix A, concurrent synchronization should occur for $\alpha > 10.25$. A simulation is shown in figure 6. One can see clearly that, after a transient period, oscillators 2, 3, 4 are in perfect sync, as well as oscillators 5, 6, 7, but that the two groups are not in sync with each other.

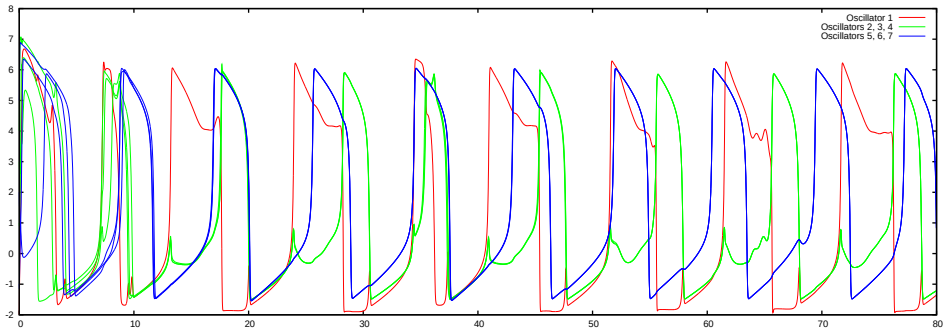

Fig. 6. Simulation result for network 3.

3.4 Robustness of synchronization

So far, we have been considering *exact* synchronization of *identical* elements. However this assumption may seem unrealistic, since real systems are never absolutely identical. We use here the robustness result for contracting systems (see theorem 2) to guarantee approximate synchronization even when the elements or the connections are not identical.

Consider, as in section 2.3, a network of n dynamical elements

$$\dot{\mathbf{x}}_i = \mathbf{f}_i(\mathbf{x}_i, t) + \sum_{j \neq i} \mathbf{K}_{ij}(\mathbf{x}_j - \mathbf{x}_i) \qquad i = 1, \ldots, n \tag{12}$$

with now possibly $\mathbf{f}_i \neq \mathbf{f}_j$ for $i \neq j$. This can be rewritten as

$$\begin{pmatrix} \dot{\mathbf{x}}_1 \\ \vdots \\ \dot{\mathbf{x}}_n \end{pmatrix} = \begin{pmatrix} \mathbf{c}(\mathbf{x}_1, t) \\ \vdots \\ \mathbf{c}(\mathbf{x}_n, t) \end{pmatrix} - \mathbf{L} \begin{pmatrix} \mathbf{x}_1 \\ \vdots \\ \mathbf{x}_n \end{pmatrix} + \begin{pmatrix} \mathbf{f}_1(\mathbf{x}_1, t) - \mathbf{c}(\mathbf{x}_1, t) \\ \vdots \\ \mathbf{f}_n(\mathbf{x}_n, t) - \mathbf{c}(\mathbf{x}_n, t) \end{pmatrix} \tag{13}$$

where $\mathbf{c}$ is some function to be defined later. Keeping the notations introduced in section 2.3, one has

$$\dot{\widehat{\mathbf{x}}} = \widehat{\mathbf{c}}(\widehat{\mathbf{x}}, t) - \mathbf{L}\widehat{\mathbf{x}} + \mathbf{d}(\widehat{\mathbf{x}}, t)$$

where $\mathbf{d}(\widehat{\mathbf{x}}, t)$ stands for the last term of equation (13).

Consider now the projected auxiliary system on $\mathcal{M}^\perp$

$$\dot{\mathbf{y}} = \mathbf{V}\widehat{\mathbf{c}}(\mathbf{V}^\top \mathbf{y} + \mathbf{U}\mathbf{U}^\top \widehat{\mathbf{x}}, t) - \mathbf{V}\mathbf{L}\mathbf{V}^\top \mathbf{y} + \mathbf{V}\mathbf{d}(\mathbf{V}^\top \mathbf{y} + \mathbf{U}\mathbf{U}^\top \widehat{\mathbf{x}}, t) \tag{14}$$

Assume that the connections represented by $\mathbf{L}$ are strong enough (in the sense of equation (10)), so that the undisturbed version of (14) is contracting with rate $\lambda > 0$. Let $D = \sup_{\widehat{\mathbf{x}},t} \|\mathbf{V}\mathbf{d}(\widehat{\mathbf{x}}, t)\|$, where D can be viewed as a measure of the dissimilarity of the elements. Since $\mathbf{y} = \mathbf{0}$ is a particular solution of the undisturbed system, theorem 2 implies that the distance $R(t)$ between any trajectory of (14) and $\mathbf{0}$ verifies, after a transient period, $R(t) \leq D/\lambda$. In the $\mathbf{x}$-space, it means that *any trajectory will eventually be contained in a boundary layer of thickness D/λ around the synchronization subspace $\mathcal{M}$.*

The choice of $\mathbf{c}$ can now be specified so as to minimize D/λ. Neglecting for simplicity the variation of λ, a possible choice for $\mathbf{c}(\mathbf{x}, t)$ is then the center of the ball of smallest radius containing $\mathbf{f}_1(\mathbf{x}, t), \ldots, \mathbf{f}_n(\mathbf{x}, t)$, with D being the radius of that ball.

Consider for instance, the following system (similar to the model used for coincidence detection in [48] and section 5.1)

$$\dot{x}_i = f(x_i) + I_i + k(x_0 - x_i) \qquad \text{where } I_{\min} \leq I_i \leq I_{\max},\ \forall i$$

In this case, choosing $c(x) = f(x) + \frac{I_{\max}+I_{\min}}{2}$, one can achieve the bound D/λ, where λ is the contraction rate of f and $D = \frac{I_{\max}-I_{\min}}{2}$.

Remark : Assume that two spiking neurons are approximately synchronized, as just discussed. Then, since spiking induces large abrupt variations, the neurons must spike approximately at the same time. More specifically, if the

bound on their trajectory discrepancy guaranteed by the above robustness result is significantly smaller than spike size, then this bound will automatically imply that the two neurons spike approximately at the same time.

4 Combinations of concurrently synchronized groups

This section shows that, under mild conditions, global convergence to a concurrently synchronized regime is preserved under basic system combinations, and thus that stable concurrently synchronized aggregates of arbitrary size can be systematically constructed. The results, derived for two groups, extend by recursion to arbitrary numbers of groups.

4.1 The input-equivalence preservation assumption

Consider two independent groups of dynamical elements, say S_1 and S_2. For each group i ($i = 1, 2$), assume that a flow-invariant subspace $\mathcal{M}_i$ corresponding to a concurrently synchronized regime exists. Assume furthermore that contraction to this subspace can be shown, i.e. $\mathbf{V}_i \mathbf{J}_i \mathbf{V}_i^\top < \mathbf{0}$ for some projection matrix $\mathbf{V}_i$ on $\mathcal{M}_i^\perp$.

Connect now the elements of S_1 to the elements of S_2, *while preserving input-equivalence* for each aspiring synchronized subgroup of S_1 and S_2. Thus, the combined concurrent synchronization subspace $\mathcal{M}_1 \times \mathcal{M}_2$ remains a flow-invariant subspace of the new global space. A projection matrix on $(\mathcal{M}_1 \times \mathcal{M}_2)^\perp$ can be $\mathbf{V} = \begin{pmatrix} \mathbf{W}_1 & \mathbf{0} \\ \mathbf{0} & \mathbf{W}_2 \end{pmatrix}$ where each $\mathbf{V}_i$ has been rescaled into $\mathbf{W}_i$ to preserve orthonormality.

Specific mechanisms facilitating input-equivalence preservation will be discussed in section 4.2.3.

4.2 Typology of combinations

Let us now study several combination operations of concurrently synchronized groups and discuss how they can preserve convergence to a combined concurrent sync state.

In 4.2.1 and 4.2.2, the input-equivalence preservation condition of section 4.1 is implicitly assumed, and the results reflect similar combination properties

of contracting systems [27,43,46]. More generally, as long as input-equivalence is preserved, any combination property for contracting systems can be easily "translated" into a combination property for synchronizing systems.

4.2.1 Negative feedback combination

The Jacobian matrices of the couplings are of the form $\mathbf{J}_{12} = -k\mathbf{J}_{21}^\top$, with k a positive constant. Thus, the Jacobian matrix of the global system can be written as

$$\mathbf{J} = \begin{pmatrix} \mathbf{J}_1 & -k\mathbf{J}_{21}^\top \\ \mathbf{J}_{21} & \mathbf{J}_2 \end{pmatrix}$$

As in equation (6) of section 2.2, consider a transform $\mathbf{\Theta}$ over $(\mathcal{M}_1 \times \mathcal{M}_2)^\perp$

$$\mathbf{\Theta} = \begin{pmatrix} \mathbf{I} & \mathbf{0} \\ \mathbf{0} & \sqrt{k}\mathbf{I} \end{pmatrix}$$

The corresponding *generalized* projected Jacobian matrix on $(\mathcal{M}_1 \times \mathcal{M}_2)^\perp$ is

$$\mathbf{\Theta}(\mathbf{V}\mathbf{J}\mathbf{V}^\top)\mathbf{\Theta}^{-1} = \begin{pmatrix} \mathbf{W}_1\mathbf{J}_1{\mathbf{W}_1}^\top & \frac{1}{\sqrt{k}}\mathbf{W}_1(-k\mathbf{J}_{21}^\top){\mathbf{W}_2}^\top \\ \sqrt{k}\mathbf{W}_2\mathbf{J}_{21}{\mathbf{W}_1}^\top & \mathbf{W}_2\mathbf{J}_2{\mathbf{W}_2}^\top \end{pmatrix} < \mathbf{0} \quad \text{uniformly}$$

so that global exponential convergence to the combined concurrent synchronization state can be then concluded.

4.2.2 Hierarchical combination

Assume that the elements in S_1 provide feedforward to elements in S_2 but do not receive any feedback from them. Thus, the Jacobian matrix of the global system is $\mathbf{J} = \begin{pmatrix} \mathbf{J}_1 & \mathbf{0} \\ \mathbf{J}_{21} & \mathbf{J}_2 \end{pmatrix}$. Assume now that $\mathbf{W}_2\mathbf{J}_{21}{\mathbf{W}_1}^\top$ is uniformly bounded and consider the coordinate transform $\mathbf{\Theta}_\epsilon = \begin{pmatrix} \mathbf{I} & \mathbf{0} \\ \mathbf{0} & \epsilon\mathbf{I} \end{pmatrix}$. Compute the

generalized projected Jacobian

$$\mathbf{\Theta}_\epsilon(\mathbf{V}\mathbf{J}\mathbf{V}^\top)\mathbf{\Theta}_\epsilon^{-1} = \begin{pmatrix} \mathbf{W}_1\mathbf{J}_1{\mathbf{W}_1}^\top & \mathbf{0} \\ \epsilon\mathbf{W}_2\mathbf{J}_{21}{\mathbf{W}_1}^\top & \mathbf{W}_2\mathbf{J}_2{\mathbf{W}_2}^\top \end{pmatrix}$$

Since $\mathbf{W}_2\mathbf{J}_{21}{\mathbf{W}_1}^\top$ is bounded, and $\mathbf{W}_1(\mathbf{J}_1){\mathbf{W}_1}^\top$ and $\mathbf{W}_2(\mathbf{J}_2){\mathbf{W}_2}^\top$ are both negative definite, $\mathbf{\Theta}_\epsilon(\mathbf{V}\mathbf{J}\mathbf{V}^\top)\mathbf{\Theta}_\epsilon^{-1}$ will be negative definite for small enough ϵ.

Note that classical graph algorithms [22] allow large system aggregates to be systematically decomposed into hierarchies (directed acyclic graphs, feedforward networks) of simpler subsystems (strongly connected components) [46]. Input-equivalence then needs only be verified top-down.

4.2.3 Case where S_1 has a single element

Denote this element by e_1 (figure 1 shows such a configuration where e_1 is the round red central element, and where S_2 is the set of the remaining elements). Connections from (resp. to) e_1 will be called 1→2 (resp. 2→1) connections. Then some simplifications can be made :

- Input-equivalence is preserved whenever, for each aspiring synchronized subgroup of S_2, the 1→2 connections are identical for each element of this subgroup (in figure 1, the connections from e_1 to the yellow diamond elements are the same). In particular, one can add/suppress/modify any 2→1 connection without altering input-equivalence.
- Since $\dim(\mathcal{M}_1^\perp) = 0$ (a single element is always synchronized with itself), one has $(\mathcal{M}_1 \times \mathcal{M}_2)^\perp = \mathcal{M}_2^\perp$. Thus, concurrent synchronization (and the rate of convergence) of the combined system only depends on the parameters and the states of the elements within S_2. In particular, it neither depends on the actual state of e_1, nor on the connections from/to e_1 (in figure 1, the black arrows towards the red central element are arbitrary).

In practice, the condition of identical 1→2 connections is quite pervasive. In a neuronal context, one neuron with high fan-out may have 10^4 identical outgoing connections.

It is therefore quite easy to preserve an existing concurrent synchonization behavior while adding groups consisting of a single element. Thus, stable concurrent synchronization can be easily built one element at a time.

4.2.4 The diffusive case

We stick with the case where S_1 consists of a single element, but make now the additionnal requirement that the 1→2 connections and the internal connections within S_2 are *diffusive* (so far in this section 4, we have implicitly assumed that the connections from S_i to S_j only involve the states of elements in S_i). The Jacobian matrix of the combined system is now of the form

$$\mathbf{J} = \begin{pmatrix} \frac{\partial g(x_1,t)}{\partial x_1} & & & \\ & \frac{\partial f_1(x_2,t)}{\partial x_2} & & \\ & & \ddots & \\ & & & \frac{\partial f_q(x_n,t)}{\partial x_n} \end{pmatrix} + \begin{pmatrix} * & * & * & * \\ k_1 & -k_1 & & \\ \vdots & & \ddots & \\ k_q & & & -k_q \end{pmatrix} - \begin{pmatrix} 0 & 0 \\ 0 & \mathbf{L}_{\text{int}} \end{pmatrix}$$

where the first matrix describes the internal dynamics of each element, the second, the diffusive connections between e_1 and S_2 (where S_2 has q aspiring synchronized subgroups), and the third, the internal diffusive connections within S_2.

Hence, the projected Jacobian matrix on $(\mathcal{M}_1 \times \mathcal{M}_2)^\perp = \mathcal{M}_2^\perp$ is

$$\mathbf{V}_2 \begin{pmatrix} \frac{\partial f_1(x_2,t)}{\partial x_2} & & \\ & \ddots & \\ & & \frac{\partial f_q(x_n,t)}{\partial x_n} \end{pmatrix} \mathbf{V}_2^\top - \mathbf{V}_2 \begin{pmatrix} k_1 & & \\ & \ddots & \\ & & k_q \end{pmatrix} \mathbf{V}_2^\top - \mathbf{V}_2 \mathbf{L}_{\text{int}} \mathbf{V}_2^\top$$

An interpretation of this remark is that there are basically three ways to achieve concurrent synchronization within S_2, *regardless of the behavior of element e_1 and of its connections* :

- **(i)** one can increase the strengths $k_1, \ldots, k_q$ of the 1→2 connections (which corresponds to adding inhibitory damping to S_2), so that each element of S_2 becomes *contracting*. In this case, all these elements will synchronize because of their contracting property even *without any direct coupling* among them ($\mathbf{L}_{\text{int}} = 0$) (this possibility of synchronization without direct coupling is exploited in the coincidence detection algorithm of [50], and again in section 5.1 of this paper),
- **(ii)** or one can increase the strength $\mathbf{L}_{\text{int}}$ of the internal connections among the elements of S_2,
- **(iii)** or one can combine the two.

4.2.5 Parallel combination

The elementary fact that, if $\mathbf{V}\mathbf{J}_i\mathbf{V}^\top < \mathbf{0}$ for a set of subsystem Jacobian matrices $\mathbf{J}_i$, then $\mathbf{V}\left(\sum_i \alpha_i(t)\mathbf{J}_i\right)\mathbf{V}^\top < \mathbf{0}$ for positive $\alpha_i(t)$, can be used in many ways. Note that it does not represent a combination of different groups as in the above paragraphs, but rather a superposition of different dynamics within one group.

One such interpretation, as in [43] for contracting systems, is to assume that for a given system $\dot{\mathbf{x}} = \mathbf{f}(\mathbf{x}, t)$, several types of additive couplings $\mathbf{L}_i(\mathbf{x}, t)$ lead stably to the *same* invariant set, but to different synchronized behaviors. Then any convex combination ($\alpha_i(t) \geq 0, \sum_i \alpha_i(t) = 1$) of the couplings will lead stably to the same invariant set. Indeed,

$$\mathbf{f}(\mathbf{x}, t) - \sum_i \alpha_i(t)\mathbf{L}_i(\mathbf{x}, t) = \sum_i \alpha_i(t)\left[\mathbf{f}(\mathbf{x}, t) - \mathbf{L}_i(\mathbf{x}, t)\right] < \mathbf{0}$$

The $\mathbf{L}_i(\mathbf{x}, t)$ can be viewed as *synchronization primitives* to shape the behavior of the combination.

5 Examples

In conclusion, let us briefly discuss some general directions of application of the above results to a few classical problems in systems neuroscience and robotics.

5.1 Coincidence detection for multiple groups

Coincidence detection is a classic mechanism proposed for segmentation and classification. In an image for instance, elements moving at a common velocity are typically interpreted as being part of a single object, and this even when the image is only composed of random dots [25,23].

As mentioned in section 4.2, the possibility of decentralized synchronization via central diffusive couplings can be used in building a coincidence detector. In [50], inspired in part by [1], the authors consider a leader-followers network of FitzHugh-Nagumo [9] oscillators, where each follower oscillator i (an element of S_2, see section 4.2.4) receives an external input I_i as well as a diffusive coupling from the leader oscillator (the element e_1 of S_1). Oscillators i and j receiving the same input ($I_i = I_j$) synchronize, so that choosing the system

[9] See appendix A.

output as $\sum_{1\leq i\leq n}[\dot{v}_i]^+$ captures the moment when a large number of oscillators receive the same input.

However, the previous development also implies that this very network can detect the moments when *several* groups of identical inputs exist. Furthermore, it is possible to identify the number of such groups and their relative size. Indeed, assume that the inputs are divided into k groups, such that for each group S_m, one has $\forall i, j \in S_m, I_i = I_j$. Since the oscillators in S_m only receive as input (a) the output of the leader, which is the same for everybody and (b) the external input I_i, which is the same for every oscillator in group S_m, they are input-symmetric and should synchronize with each other (cf. section 3.2 and section 4.2.4).

Some simulation results are shown in figure 7. Note that contrast between groups could be further enhanced by using nonlinear "synapses", e.g. introducing input-dependent delays, which would preserve the symmetries. Similarly, any feedback mechanism to the leader oscillator would also preserve the input-symmetries.

Finally, adding all-to-all identical connections between the follower oscillators would preserve the input-symmetries and further increase the convergence rate, but at the price of vastly increased complexity.

5.2 Fast symmetry detection

Symmetry, in particular bilateral symmetry, has also been shown to play a key role in human perception [3]. Consider a group of oscillators having the same individual dynamics and connected together in a symmetric manner. If we present to the network an input having the same symmetry, some of the oscillators will synchronize as predicted by the theoretical results of section 3.2.

One application of this idea is to build a fast bilateral symmetry detector (figures 8, 9, 10), extending the oscillator-based coincidence detectors of the previous section. Although based on a radically different mechanism, this symmetry detector is also somewhat reminiscent of the device in [3].

Some variations are possible :

- **(i)** *Other types of invariance.* It is easy to modify the network in order to deal with multi-order (as opposed to bilateral) symmetry, or other types of invariance (translation, rotation, ...). In each case, the network should have the same invariance pattern as what it is supposed to detect.
- **(ii)** Since the exponential convergence rate is known, the network may be used

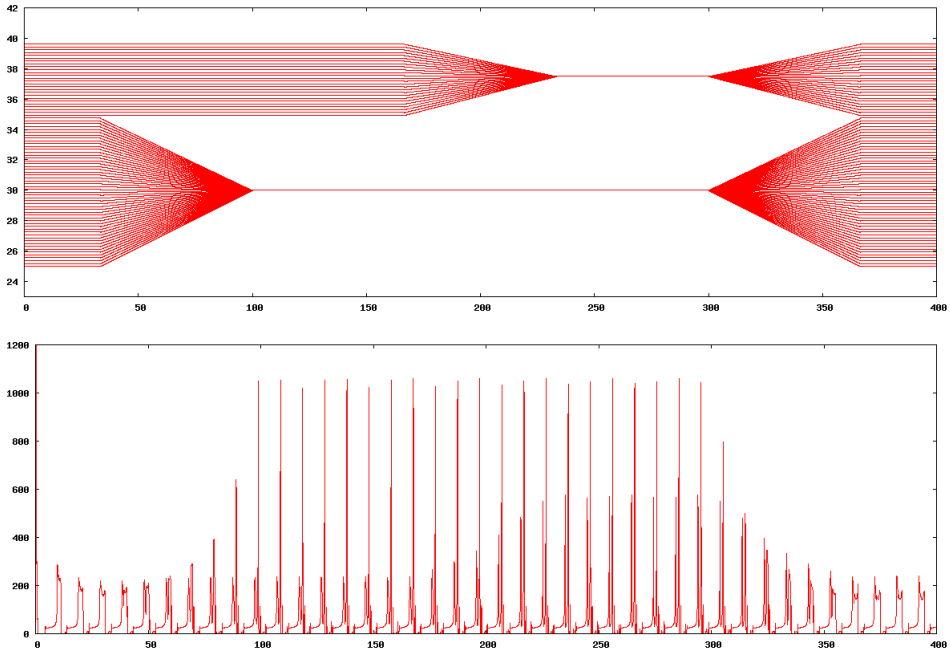

Fig. 7. Simulation results for the coincidence detector. The network is composed of one leader with a constant input $I_0 = 25$, and 80 followers whose inputs vary with time as shown in the upper figure. The lower figure plots the system output $\left(\sum_{1\leq i\leq 80}[\dot{v}_i]^+\right)$ against time. One can clearly observe the existence of two successive, well separated spikes per period in a time interval around $t = 250$. Furthermore, one spike is about twice as large as the other one. This agrees with the inputs, since around $t = 250$, they are divided into two groups : 1/3 of them with value 37, 2/3 with value 30.

to track *time-varying* inputs, as in the coincidence detection algorithm of [50], or to detect transient coincidence as in Fig. 10.

(iii) *Multidimensional inputs.* Coincidence detectors and symmetry detectors may also handle multidimensional inputs. Two approaches are possible. One can either "hash" each multidimensional input into a one-dimensional input, and give the set of so-obtained one-dimensional inputs to the network. Or one can process each dimension independently in separate networks and then combine the results in a second step.

5.3 Central pattern generators

In an animal/robotics locomotion context, central pattern generators are often modelled as coupled nonlinear oscillators delivering phase-locked signals. We consider here a system of three coupled 2-dimensional Andronov-Hopf oscillators [18], very similar to the ones used in the simulation of salamander

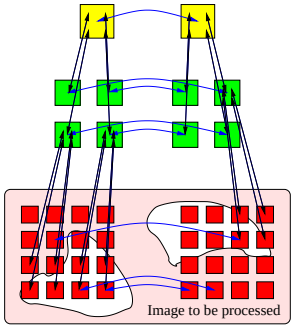

Fig. 8. A fast bilateral symmetry detector.
Every oscillator has the same dynamics as its mirror image and the two are coupled through diffusive connection. The inputs are provided to the detector through the bottom (red) layer. Then "information" travels bottom-up : each layer is connected to the layer right above it. Top-down feedback is also possible.
Assume now that a mirror symmetric image is submitted to the network. The network, which is mirror symmetric by construction, now receives a mirror symmetric input. Thus, the concurrent synchronization subspace where each oscillator is exactly in the same state as its mirror image oscillator is flow-invariant. Furthermore, the diffusive connections, if they are strong enough (see 2.2), guarantee contraction on the orthogonal space. By using the theoretical results above, one can deduce the exponential convergence to the concurrent synchronization regime. In particular, the difference between the top two oscillators should converge exponentially to zero.

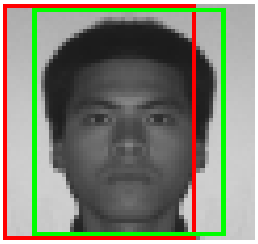

Fig. 9. Simulation on an artificial image.
We create a 56×60 pixels symmetric image from a real picture of one of the authors. We give it as input to a network similar to the one in figure 8. The first (bottom) layer of the network is composed of $7 \times 6 = 42$ FitzHugh-Nagumo oscillators (21 pairs) each receiving the sum of the intensities of $8 \times 8 = 64$ pixels, thus covering at every instant an active window of 56×48 pixels. The second layer consists of 4 oscillators, each receiving inputs from 9 or 12 oscillators of the first layer. The third layer is composed of 2 oscillators. At $t = 0$, the active window is placed on the left of the image (red box) and, as t increases, it slides towards the right. At $t = T/2$, where T is the total time of the simulation, the position of the window is exactly at the center of the image (green box) (see the simulation results in figure 10).

locomotion [15] :

$$\begin{cases} \dot{\mathbf{x}}_1 = \mathbf{f}(\mathbf{x}_1) + k(\mathbf{R}_{\frac{2\pi}{3}}\mathbf{x}_2 - \mathbf{x}_1) \\ \dot{\mathbf{x}}_2 = \mathbf{f}(\mathbf{x}_2) + k(\mathbf{R}_{\frac{2\pi}{3}}\mathbf{x}_3 - \mathbf{x}_2) \\ \dot{\mathbf{x}}_3 = \mathbf{f}(\mathbf{x}_3) + k(\mathbf{R}_{\frac{2\pi}{3}}\mathbf{x}_1 - \mathbf{x}_3) \end{cases}$$

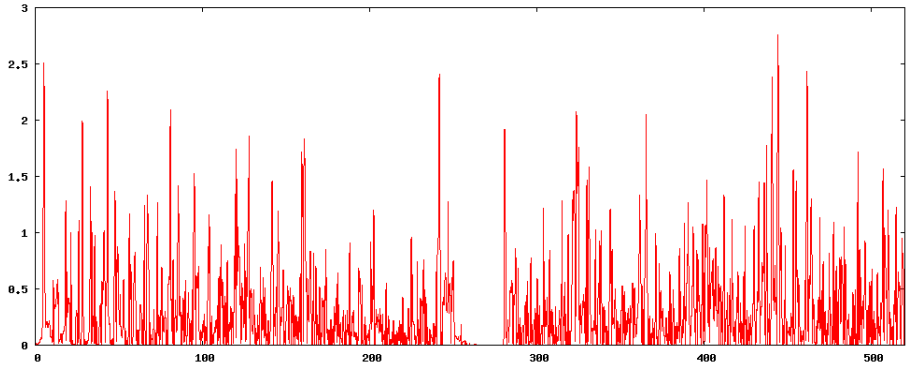

Fig. 10. Result for the simulation of figure 9. The figure shows $|v_1 - v_2|$ where v_1 and v_2 are the voltages of the two FN oscillators in the top layer. One can clearly observe that, around $t = T/2$ ($T = 520$ in this simulation), there is a short time interval during which the two oscillators are fully synchronized.

where $\mathbf{f}$ is the dynamics of an Andronov-Hopf oscillator and the matrix $\mathbf{R}_{\frac{2\pi}{3}}$ describes a $\frac{2\pi}{3}$ planar rotation :

$$\mathbf{f}\begin{pmatrix} x \\ y \end{pmatrix} = \begin{pmatrix} x - y - x^3 - xy^2 \\ x + y - y^3 - yx^2 \end{pmatrix} \qquad \mathbf{R}_{\frac{2\pi}{3}} = \begin{pmatrix} -\frac{1}{2} & -\frac{\sqrt{3}}{2} \\ \frac{\sqrt{3}}{2} & -\frac{1}{2} \end{pmatrix}$$

We can rewrite the dynamics as $\dot{\widehat{\mathbf{x}}} = \widehat{\mathbf{f}}(\widehat{\mathbf{x}}) - k\mathbf{L}\widehat{\mathbf{x}}$, where

$$\mathbf{L} = \begin{pmatrix} \mathbf{I}_2 & -\mathbf{R}_{\frac{2\pi}{3}} & \mathbf{0} \\ \mathbf{0} & \mathbf{I}_2 & -\mathbf{R}_{\frac{2\pi}{3}} \\ -\mathbf{R}_{\frac{2\pi}{3}} & \mathbf{0} & \mathbf{I}_2 \end{pmatrix}$$

First, observe that the *linear* subspace $\mathcal{M} = \left\{ \left(\mathbf{R}^2_{\frac{2\pi}{3}}(\mathbf{x}), \mathbf{R}_{\frac{2\pi}{3}}(\mathbf{x}), \mathbf{x} \right) : \mathbf{x} \in \mathbb{R}^2 \right\}$ is flow-invariant [10] , and that $\mathcal{M}$ is also a subset of $\mathrm{Null}(\mathbf{L}_s)$. Next, remark that the characteristic polynomial of $\mathbf{L}_s$ is $X^2\,(X - 3/2)^4$ so that the eigenvalues of $\mathbf{L}_s$ are 0, with multiplicity 2, and 3/2, with multiplicity 4. Now since $\mathcal{M}$ is 2-dimensional, it is exactly the nullspace of $\mathbf{L}_s$, which implies in turn that $\mathcal{M}^\perp$ is the eigenspace corresponding to the eigenvalue 3/2.

Moreover, the eigenvalues of the symmetric part of $\widehat{\frac{\partial \mathbf{f}}{\partial \mathbf{x}}}(x, y)$ are $1-(x^2+y^2)$ and $1-3(x^2+y^2)$, which are upper-bounded by 1. Thus, for $k > 2/3$ (see equation (10) in section 2.3), the three systems will *globally exponentially converge to a* $\pm\frac{2\pi}{3}$*-phase-locked state* (i. e. a state in which the difference of the phases of

[10] As it is suggested in footnote 7, the flow-invariance of $\mathcal{M}$ can be understood here as being "created" by the internal symmetries of the oscillators' dynamics.

two consecutive elements is constant and equals $\pm\frac{2\pi}{3}$). A computer simulation is presented in figure 11.

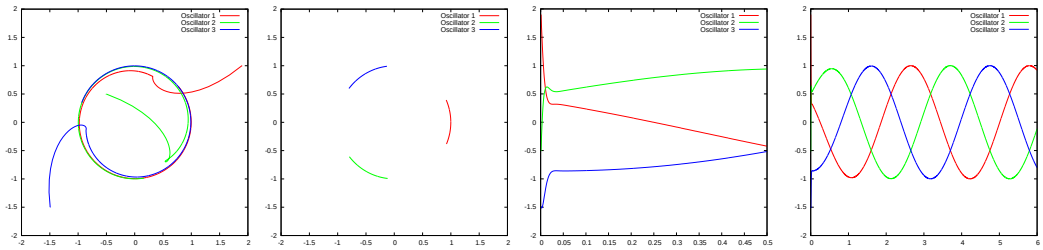

Fig. 11. Simulation for three coupled Andronov-Hopf oscillators. In the first two figures, we plot y_i against x_i for $1 \leq i \leq 3$. Figure a shows the behavior of the oscillators for $0 \leq t \leq 3s$, figure b for $5.6s \leq t \leq 6s$. In figures c and d, we plot x_1, x_2, x_3 against time. Figure c for $0 \leq t \leq 0.5s$, figure d for $0 \leq t \leq 6s$.

Relaxing the symmetry or the diffusivity condition : In the previous example, the flow-invariance of the phase-locked state is due to (a) the internal symmetry of the individual dynamics $\mathbf{f}$, (b) the global symmetry of the connections and (c) the "diffusivity" of the connections (of the form $k(\mathbf{R}\mathbf{x}_2 - \mathbf{x}_1)$). Observe now, as in section 3.2, that this flow-invariance can be preserved when one out of the two conditions (b) and (c) is relaxed. Consider for example the two following systems :

- Symmetric but not "diffusive" :

$$\begin{cases} \dot{\mathbf{x}}_1 = \mathbf{f}(\mathbf{x}_1) + k\mathbf{R}_{\frac{2\pi}{3}}\mathbf{x}_2 \\ \dot{\mathbf{x}}_2 = \mathbf{f}(\mathbf{x}_2) + k\mathbf{R}_{\frac{2\pi}{3}}\mathbf{x}_3 \\ \dot{\mathbf{x}}_3 = \mathbf{f}(\mathbf{x}_3) + k\mathbf{R}_{\frac{2\pi}{3}}\mathbf{x}_1 \end{cases}$$

  (the connections are "excitatory-only" in the sense of section 3.1.3).
- "Diffusive" but not symmetric :

$$\begin{cases} \dot{\mathbf{x}}_1 = \mathbf{f}(\mathbf{x}_1) + k_1(\mathbf{R}_1\mathbf{x}_2 - \mathbf{x}_1) \\ \dot{\mathbf{x}}_2 = \mathbf{f}(\mathbf{x}_2) + k_2(\mathbf{R}_2\mathbf{x}_3 - \mathbf{x}_2) \\ \dot{\mathbf{x}}_3 = \mathbf{f}(\mathbf{x}_3) + k_3(\mathbf{R}_3\mathbf{x}_1 - \mathbf{x}_3) \end{cases}$$

  where the $\mathbf{R}_i$ represent any planar rotations such that $\mathbf{R}_1\mathbf{R}_2\mathbf{R}_3 = \mathbf{I}_2$ (i.e., any arbitrary phase-locking).

By keeping in mind that for any planar rotation $\mathbf{R}$ and state $\mathbf{x}$, one has $\mathbf{f}(\mathbf{R}\mathbf{x}) = \mathbf{R}(\mathbf{f}(\mathbf{x}))$, it is immediate to show the flow-invariance of $\left\{\left(\mathbf{R}^2_{\frac{2\pi}{3}}(\mathbf{x}), \mathbf{R}_{\frac{2\pi}{3}}(\mathbf{x}), \mathbf{x}\right) : \mathbf{x} \in \mathbb{R}^2\right\}$ in the first case, and of $\{(\mathbf{R}_1\mathbf{R}_2(\mathbf{x}), \mathbf{R}_1(\mathbf{x}), \mathbf{x}) : \mathbf{x} \in \mathbb{R}^2\}$ in the second case. Note however that the computations of the projected Jacobian matrices are

different, and that in the first case the limit cycle's radius varies with k (cf. section 3.1.3).

Finally, note that

(i) All the results of this section can be immediately extended to systems with more oscillators.

(ii) As compared to results based only on phase oscillators, this analysis guarantees global exponential convergence, rather than assuming that synchronization is already essentially achieved. In addition, it exhibits none of the topological difficulties that may arise when coupling large numbers of phase oscillators.

(iii) If $\mathbf{f}$ is less symmetric, only connections that exhibit the same symmetry as $\mathbf{f}$ can lead to a non-trivial flow-invariance subspace.

(iv) It is also possible to extend this study to systems composed of oscillators with larger dimensions (living in $\mathbb{R}^3$ for example), although a locomotion interpretation may be less relevant.

5.4 Filtered connections and automatic gait selection

Replacing ordinary connections in the CPG described in section 5.3 by filters enables *frequency-based symmetry selection*. This idea may have powerful applications, one of which could be automatic gait selection in locomotion.

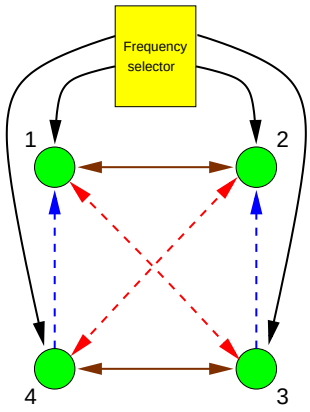

Fig. 12. A CPG with filtered connections. The connections from the command box set the same frequency for the four oscillators. The $1 \leftrightarrow 2$ and $3 \leftrightarrow 4$ arrows represent permanent *anti-synchronization* connections (i.e. connection $j \to i$ is of the form $k(-\mathbf{x}_j - \mathbf{x}_i)$). The $1 \leftrightarrow 3$ and $2 \leftrightarrow 4$ arrows represent *synchronization* connections and they are *high-pass* filtered. Finally, the $3 \to 2$ and $4 \to 1$ arrows stand for *quarter-period delay* connections (i.e. connection $j \to i$ is of the form $k(\mathbf{R}_{-\frac{\pi}{2}}\mathbf{x}_j - \mathbf{x}_i)$, see section 5.3) and they are *low–pass* filtered.

Consider for example the mechanism described in figure 12. At low frequencies, the $1 \leftrightarrow 3$ and $2 \leftrightarrow 4$ connections are filtered out, so that the actual connections are $1 \leftrightarrow 2$ and $3 \leftrightarrow 4$ (anti-synchronization) and $3 \to 2$ and $4 \to 1$ (quarter-period delay). The only non-trivial flow-invariant subspace is then $\{\mathbf{x}_1 = \mathbf{R}_{\frac{\pi}{2}}(\mathbf{x}_3) = -\mathbf{x}_2 = \mathbf{R}_{\frac{3\pi}{2}}(\mathbf{x}_4)\}$. On the contrary, the $3 \to 2$ and $4 \to 1$ connections are filtered out at high frequencies, so that the flow-invariant subspace becomes $\{\mathbf{x}_1 = \mathbf{x}_3 = -\mathbf{x}_2 = -\mathbf{x}_4\}$.

Similarly to section 5.3, strong enough coupling gains ensure convergence to either of these two subspaces, according to the frequency at which the oscillators are running. Note that standard techniques allow sharp causal filters with frequency-independent delays to be constructed easily [34].

An analogy with horse gaits could be made in this simplified setup, by associating the low-frequency regime with the *walk* (left fore, right hind, right fore, left hind), and the high-frequency regime with the *trot* (left fore and right hind simultaneously, then right fore and left hind simultaneously). Transitions between the two regimes would occur automatically according to the speed of the horse (the frequency of its gait).

5.5 Temporal binding

The previous development has suggested a mechanism for stable accumulation and interaction of concurrently synchronized groups, showing that the simple conditions for contraction to a linear subspace, combined with the high fan-out of typical neurons, increased the plausibility of large concurrently synchronized structures being created in the central nervous system in the course of evolution and development. The recently established pervasiveness of electrical synapses [9] would also be consistent with such architectures.

More speculatively, different "rhythms" ($\alpha, \beta, \gamma, \delta$) are known to coexist in the brain, which, in the light of the previous analysis, may be interpreted and modelled as concurrently synchronized regimes. Since contracting systems driven by periodic inputs will have states of the same period [27], different but synchronized computations could be robustly carried out by specialized areas in the brain using synchronized elements as their inputs. Such a temporal "binding" [42,13,25,47,23,32,51,4,9] mechanism would also complement the general argument in [44] that multisensory integration may occur through the interaction of contracting computational systems connected through an extensive network of feedback loops. In this context, and along the lines of section 4.2, a translation to concurrent synchronization of recent results on centralized contracting combinations [46] may be particularly relevant, as could be frequency-based selection mechanisms. Making these observations precise is the subject of future research.

Acknowledgments

We are grateful to Jake Bouvrie, Nicolas Tabareau and Sacha Zyto for stimulating discussions, and to an anonymous reviewer for thoughtful suggestions

to improve the presentation. The first author would like to thank CROUS, Paris for financial support.

A FitzHugh-Nagumo oscillators

Some of our simulations involve coupled FitzHugh-Nagumo neural oscillators [8,31]

$$\begin{cases} \dot{v}_i = v_i(\alpha - v_i)(v_i - 1) - w_i + I_i + k(v_0 - v_i) \\ \dot{w}_i = \beta v_i - \gamma w_i \end{cases} \qquad 1 \leq i \leq n$$

In this paper, we use the following parameters values : $\alpha = 6,\ \beta = 3,\ \gamma = 0.09$.

The contraction analysis of FitzHugh-Nagumo oscillators can be adapted from [48].

References

[1] C. Brody, J. Hopfield. Simple Networks for Spike-Timing-Based Computation, with Application to Olfactor Processing. *Neuron*, **37** (5):843–852, 2003.

[2] V. Belykh, I. Belykh, M. Hasler, K. Nevidin. Cluster Synchronization in Three-dimensional Lattices of Diffusively Coupled Oscillators. *Int. J. of Bifurcation and Chaos*, **13**:755–779, 2003.

[3] V. Braitenberg. *Vehicles: Experiments in Synthetic Psychology*, chap. 9. The MIT Press, 1984.

[4] F. Crick, C. Koch. What is the Function of the Claustrum. *Phil. Trans. Roy. Soc. Lond. B*, **360**:1271–1279, 2005.

[5] P. Dayan, G. Hinton, R. Neal, R. Zemel. The Helmholtz Machine. *Neural Computation*, **7**, 1995.

[6] B. Dionne, M. Golubitsky, I. Stewart. Coupled cells with internal symmetry. *Nonlinearity*, **9**:559–599, 1996.

[7] M. Fiedler. Algebraic Connectivity of Graphs. *Czechoslovak Mathematical Journal*, 1976.

[8] R. FitzHugh. Impulses and Physiological States in Theoretical Models of Nerve Membrane. *Biophys. Journal*, **1**:445-466, 1961.

[9] T. Fukuda, T. Kosaka, W. Singer and R.A.W. Galuske. Gap Junctions among Dendrites of Cortical GABAergic Neurons Establish a Dense and Widespread Intercolumnar Network. *The Journal of Neuroscience*, **26** (13):3434–3443, 2006.

[10] D. George, J. Hawkins. Invariant Pattern Recognition using Bayesian Inference on Hierarchical Sequences, Dept. of Electrical Engineering, Stanford University, 2005.

[11] M. Golubitsky, I. Stewart. Synchrony versus Symmetry in Coupled Cells. *Equadiff 2003: Proceedings of the International Conference on Differential Equations*.

[12] M. Golubitsky, I. Stewart, A. Török. Patterns of Symmetry in Coupled Cell Networks with Multiple Arrows. *SIAM J. Appl. Dynam. Sys.*, **4** (1):78–100, 2005.

[13] S. Grossberg. The Complementary Brain : a Unifying View of Brain Specialization and Modularity. *Trends in Cognitive Sciences*, **4**:233–246, 2000.

[14] R. Horn, C. Johnson. *Matrix Analysis*. Cambridge University Press, 1985.

[15] A. Ijspeert, A. Crespi, J.-M. Cabelguen. Simulation and Robotic Studies of Salamander Locomotion : Applying Neurobiological Principles to the Control of Locomotion in Robots, 2005.

[16] E. Izhikevich. Simple Model of Spiking Neuron. *IEEE Trans. on Neural Networks*, **14**(6):1569–1572, 2003.

[17] E. Izhikevich, N. Desai, E. Walcott, F. Hoppensteadt. Bursts as a Unit of Neural Information : Selective Communication via Resonance. *Trends in Neuroscience*, **26** (3):161–167, 2003.

[18] E. Izhikevich, Y. Kuramoto. Weakly Coupled Oscillators. *Encyclopedia of Mathematical Physics*. Elsevier, 2006.

[19] A. Jadbabaie, J. Lin, A. Morse. Coordination of Groups of Mobile Autonomous Agents using Nearest Neighbor Rules. *IEEE Transactions on Automatic Control*, **48**:988–1001, 2003.

[20] A. Jadbabaie, N. Motee, M. Barahona. On the Stability of the Kuramoto Model of Coupled Nonlinear Oscillators. *Proceedings of the American Control Conf.*, Boston, MA June 30–July 2, 2004.

[21] E. Kandel, J. Schwartz, T. Jessel. *Principles of Neural Science*, 5th ed., McGraw-Hill, 2006.

[22] D. Knuth. *The Art of Computer Programming*, 3rd Ed. Addison-Wesley, 1997.

[23] C. Koch. *The Quest for Consciousness*. Roberts and Company Publishers, 2004.

[24] E. Körner, M.-O. Gewaltig, U. Körner, A. Richter, T. Rodemann. A model of computation in neocortical architecture. *Neural Networks*, **12** (7-8):989–1005, 1999.

[25] R. Llinas, E. Leznik, F. Urbano. Temporal Binding via Cortical Coincidence Detection. *PNAS*, **99** (1):449–454, 2002.

[26] Z. Lin, M. Broucke, B. Francis. Local Control Strategies for Groups of Mobile Autonomous Agents. *IEEE Trans. on Automatic Control*, **49**(4):622–629, 2004.

[27] W. Lohmiller, J.-J. Slotine. On Contraction Analysis for Nonlinear Systems. *Automatica*, **34** (6):671–682, 1998.

[28] W. Lohmiller, J.-J. Slotine. Nonlinear Process Control Using Contraction Theory. *A.I.Ch.E. Journal*, **46**(3):588-597, 2000.

[29] M. Luettgen, A. Willsky. Likelihood Calculation for a Class of Multiscale Stochastic Models, with Application to Texture Discrimination. *IEEE Transactions on Image Processing*, **4**(2):194–207, 1995.

[30] V. Mountcastle. The Cerebral Cortex. *Harvard University Press*, 1998.

[31] J. Nagumo, S. Arimoto, S. Yoshizawa. An Active Pulse Transmission Line Simulating Nerve Axon. *Proc. Inst. Radio Engineers*, **50**:2061–2070, 1962.

[32] J. Niessing, B. Ebisch, K.E. Schmidt, M. Niessing, W. Singer, R.A. Galuske. Hemodynamic Signals Correlate Tightly with Synchronized Gamma Oscillations. *Science*, **309** 948–951, 2005.

[33] R. Olfati-Saber, R. Murray. Consensus Problems in Networks of Agents With Switching Topology and Time-Delays. *IEEE Transactions on Automatic Control*, **49**(9):1520-1533, 2004.

[34] A. Oppenheim, R. Schafer, J. Buck. *Discrete-Time Signal Processing, 2nd Edition*. Prentice-Hall,1999.

[35] Q.-C. Pham, J.-J. Slotine. Attractors. *MIT-NSL Report 0505*, May 2005.

[36] A. Pogromsky, G. Santoboni, H. Nijmeijer. Partial Synchronization : from Symmetry towards Stability. *Physica D*, **172** (1-4):65–87, 2002.

[37] R. Rao, D. Ballard. Predictive Coding in the Visual Cortex. *Nature Neuroscience*, **2** (1):9–10, 1999.

[38] R. Rao. Bayesian Inference and Attention in the Visual Cortex. *Neuroreport*, **16**(16):1843–1848, 2005.

[39] A. Schnitzler, J. Gross. Normal and Pathological Oscillatory Communication in the Brain. *Nat. Rev. Neurosci.*, **6**, 285–296, 2005.

[40] J.-M. Schoffelen, R. Oostenveld, P. Fries. Neuronal Coherence as a Mechanism of Effective Corticospinal Interaction. *Science*, **308**:111–113, 2005.

[41] A. Sherman, J. Rinzel. Model for Synchronization of Pancreatic I3-cells by Gap Junction coupling. *Biophys. Journal*, **59**:547–559, 1991.

[42] W. Singer, C. Gray. Visual Feature Integration and the Temporal Correlation Hypothesis. *Annu. Rev. Neurosci.*, **18**:555–586, 1995.

[43] J.-J. Slotine. Modular Stability Tools for Distributed Computation and Control. *Int. J. Adaptive Control and Signal Processing*, **17** (6):397–416, 2003.

[44] J.-J. Slotine, W. Lohmiller. Modularity, Evolution, and the Binding Problem : A View from Stability Theory. *Neural Networks*, **14**(2):137–145, 2001.

[45] S. Strogatz. From Kuramoto to Crawford : Exploring the Onset of Synchronization in Populations of Coupled Oscillators. *Physica D*, **143** (1-4):1–20, 2000.

[46] N. Tabareau, J.-J. Slotine. Notes on Contraction Theory. *MIT-NSL Report 0503*, March 2005.

[47] G. Tononi, et al. *Proc. Natl. Acad. Sci. USA* **95**:3198–3203, 1998.

[48] W. Wang, J.-J. Slotine. On Partial Contraction Analysis for Coupled Nonlinear Oscillators. *Biological Cybernetics*, **92** (1):38–53, 2005.

[49] W. Wang, J.-J. Slotine. Contraction Analysis of Time-Delayed Communications Using Simplified Wave Variables. PS/0512070, 25 Dec 2005.

[50] W. Wang, J.-J. Slotine. Fast Computation with Neural Oscillators. *Neurocomputing*, **63**, 2005.

[51] A. Yazdanbakhsh, S. Grossberg. Fast Synchronization of Perceptual Grouping in Laminar Visual Cortical Circuits. *Neural Networks*, **17** (5-6):707–718, 2004.

[52] Y. Zhang, et al. Partial Synchronization and Spontaneous Spatial Ordering in Coupled Chaotic Systems. *Phys. Rev. E*, **63**:026211, 2001.